Numerical Methods in Civil Engineering, 11-1 (2026) 01-29



Numerical Methods in Civil Engineering

Journal Homepage: https://nmce.kntu.ac.ir/

Seismic life cycle cost assessment of buried gas pipelines using a stochastic multi-scenario probabilistic framework

Sayyed Hadi Alavi*, Mohammadreza Mashayekhi**

ARTICLE INFO

RESEARCH PAPER

Article history:
Received:
December 2025
Revised:
May 2026
Accepted:
July 2026

Keywords:
Seismic life cycle cost,
Buried pipeline,
Stochastic scenario-based,
Multi-seismic hazard

Abstract:

This study presents a stochastic scenario-based framework for evaluating the seismic life cycle cost (SLCC) of buried pipelines. Existing seismic assessment methods commonly focus on predefined hazard levels and isolated earthquake events, often neglecting the cumulative impacts of both frequent and rare earthquakes during the service life of a pipeline. Such simplifications may lead to an underestimation of the overall seismic risk and associated economic consequences. In contrast, the proposed methodology incorporates multiple stochastic seismic scenarios and explicitly accounts for uncertainties in earthquake magnitude, occurrence frequency, source location, and ground motion characteristics. The framework also accounts for uncertainty in pipeline vulnerability and damage behavior, enabling a more realistic and comprehensive estimation of potential seismic losses. To demonstrate the applicability of the proposed framework, an Iranian gas transmission pipeline is selected as a case study. The SLCC is evaluated using a probabilistic approach that propagates uncertainty through seismic hazard, vulnerability, and immediate consequence models. Furthermore, probability density functions and cumulative distribution functions of the SLCC are derived to quantify the probability of various levels of economic loss under different seismic scenarios. The results indicate that the probability of the SLCC exceeding $4 million is lower than 5%, while losses below $1 million have a probability greater than 80%. Considering all seismic sources simultaneously, the upper bound of expected losses exceeds $4.5 million. Sensitivity analysis reveals that the breakage damage ratio has the strongest influence on SLCC, producing variations between approximately −42% and +16% overall.

1. Introduction

In recent years, SLCC has been used to quantify earthquake-related damages over the lifespan of civil engineering systems [1]. This approach estimates the costs of repair, rehabilitation, and replacement, providing a long-term perspective on the economic consequences of seismic events. SLCC is especially important in regions with high seismic variability, where secondary hazards and inherent uncertainties affect the performance, safety, and sustainability of infrastructure over time [2, 3].

Buried pipelines are a critical infrastructure that demands careful evaluation. Their wide spatial distribution across areas with varying seismic and geotechnical conditions introduces significant uncertainty. As vital lifeline systems, ensuring their continuous operation is essential for public services [4, 5]. Therefore, applying SLCC analysis is particularly valuable, as it provides a comprehensive framework to assess the potential impacts of earthquakes on buried pipelines [6].

Identifying the various factors that contribute to a reasonable estimation of SLCC is the first step in the SLCC process [7]. Accurate estimation of earthquake-related losses requires a comprehensive framework that combines seismic hazard analysis, vulnerability assessment, and the quantification of vulnerability within the broader context of seismic risk [8].

* *Department of Civil Engineering, K. N. University of Technology, Tehran, Iran.*
** *Corresponding author: Assistant Professor, Department of Civil Engineering, K. N. University of Technology, Tehran, Iran. Email:m.mashayekhi@kntu.ac.ir*

https://doi.org/10.66224/NMCE.2512.1120

Buried pipelines are highly vulnerable to various seismic hazards during their service life, including the direct impacts of transient ground deformations (TGD) and secondary effects such as liquefaction, landslides, and faulting caused by permanent ground deformations (PGD) [9]. Since the early 20th century, numerous cases of severe pipeline damage following earthquakes have been documented, highlighting the critical need for seismic performance assessment [10, 11]. Previous research has employed analytical and numerical methods to investigate pipeline response [12], considering key factors such as soil conditions [13, 14], fault mechanisms [15, 16], and PGD hazards, including landslides [17, 18] and soil liquefaction [19, 20]. Seismic vulnerability of buried pipelines is commonly expressed in terms of repair rate (R_R) as a function of earthquake intensity [21]. Various studies have explored pipeline vulnerability under TGD [22, 23] and PGD hazards [24]. However, most of these studies assume a fixed or single-level seismic hazard, implicitly treating hazard and vulnerability as unchanging over time [25, 26]. This makes it difficult to capture the combined effects of multiple earthquakes, variations in seismic demand, and long-term economic impacts of damage, limiting their usefulness in SLCC. Moreover, factors such as corrosion, soil settlement, and accidental damage gradually weaken pipelines, increasing their vulnerability to earthquake shaking throughout their service life [27, 28].

To address these challenges, it is crucial to comprehensively estimate earthquake-induced losses by connecting predicted damages to both direct repair costs and wider economic impacts [29]. Various methods are available for estimating SLCC, differing in complexity, data requirements, and approaches to uncertainty [30]. These include analytical methods, scenario-based frameworks, and probabilistic simulations, which can be performed using intensity-based, scenario-based, or time-based approaches [31]. Some methods employ fragility or vulnerability models to relate earthquake intensity to expected damage and costs. For instance, Alavi and Mashayekhi [29] proposed a framework that integrates seismic hazard, pipeline vulnerability, and economic consequences into a unified risk-based SLCC formulation for buried pipelines. Similarly, Adineh et al. [32] introduced an alternative approach for estimating pipeline life-cycle costs by developing fragility curves to quantify damage and associated losses. In the traditional SLCC approach, future earthquake losses by considering only a small number of seismic intensity levels, such as maximum considered events, along with approximate probabilities and simplified estimates of repair or replacement costs [33]. These costs are usually discounted to present value and added to the initial investment, while uncertainties in seismic hazard, structural response, and damage consequences are largely overlooked [34]. Expected annual costs are often estimated using simplified damage curves that relate seismic intensity to repair or replacement costs. In essence, this method relies on closed-form probabilistic expressions to directly estimate the expected economic impact over the asset's service life [35].

An alternative approach explicitly accounts for multiple seismic scenarios throughout the pipeline's service life. Unlike traditional methods, scenario-based approaches capture the full variability of earthquake magnitudes, frequencies, locations of earthquakes, and ground motions [36]. This framework enables a more realistic and physically consistent evaluation of seismic losses by explicitly capturing the cumulative effects of repeated earthquake events on pipeline response and damage accumulation. This allows for a more realistic and physically grounded assessment of seismic loss estimation by accounting for the cumulative impact of multiple events on pipeline performance and long-term costs, thereby enabling the determination of SLCC [37]. Furthermore, uncertainty is inherent in SLCC assessment due to the stochastic nature of earthquakes, variable ground motions, and diverse pipeline responses. Traditional approaches often oversimplify these uncertainties, potentially underestimating risk and costs. Stochastic scenario-based methods account for incorporating uncertainties in seismic hazard, pipeline vulnerability, and repair costs, providing a more robust and reliable approach for estimating SLCC [38]. These approaches have also been employed for generating strong ground motion records [39] and the development of regional risk assessment frameworks [38].

This study presents a novel methodology for estimating the SLCC of buried pipelines under multiple earthquake hazards. The approach combines stochastic scenario-based modeling with probabilistic formulations across all stages of SLCC, explicitly incorporating uncertainties in seismic hazard, structural vulnerability, and loss estimation to quantify the cumulative economic impact of earthquake-induced damages over the pipeline's service life. Using the HAZUS framework [40], multiple potential earthquake hazards, including TGD and PGD, are simulated across diverse scenarios to evaluate corresponding repair and replacement costs. To illustrate its practical application, the methodology is applied to evaluate the probabilistic SLCC of a buried pipeline in southern Iran. The SLCC of the pipeline is assessed by considering the frequency, location, and intensity of seismic sources, with the exceedance probability curve providing a quantitative measure of potential losses over the pipeline's service life. While probabilistic seismic hazard analysis provides long-term expected hazard estimates representing average seismic demand, scenario-based methods enable the explicit simulation of specific earthquake events and their direct

impacts on pipeline SLCC. The main contributions of this study are summarized as follows:

- A stochastic scenario-based SLCC framework is developed that simulates multiple earthquake events over the pipeline's service life, capturing cumulative seismic losses.
- Combined modeling of TGD and PGD hazards within a unified probabilistic formulation provides a more realistic representation of seismic impacts on buried pipelines.
- Full propagation of uncertainties in seismic hazard, pipeline vulnerability, and repair costs enhances the reliability of SLCC estimates.
- Probabilistic loss-exceedance curves are generated to provide a quantitative and risk-informed basis for the long-term economic evaluation of pipeline performance.

For guidance, the structure of this paper is as follows. Section 2 presents the proposed methodology, which is complemented by probabilistic models in Section 3. Section 4 introduces a case study to demonstrate the application of the methodology, while Section 5 presents the corresponding results. A brief discussion of the proposed approach is provided in Section 6, and conclusions are drawn in Section 7.

2. The proposed framework

This section presents the proposed framework for quantifying the SLCC of buried pipelines using stochastic scenario-based seismic analysis. Because the approach relies on scenario-driven earthquake distributions, the selection and treatment of scenarios significantly influence the resulting SLCC estimates. A detailed description of the stochastic scenario-based methodology is provided below.

In brief, a step-by-step graphical representation of the proposed framework is shown in Figure 1. The framework comprises four main stages: (1) seismic scenario hazard simulation, (2) seismic vulnerability assessment, (3) seismic loss estimation, and (4) SLCC estimation. In the first stage, earthquake events over the service life of the pipeline are simulated using the proposed scenario-based approach, and the associated TGD and PGD hazards are quantified. In the following seismic vulnerability assessment stage, the extent of damage along the pipeline caused by TGD and PGD for each simulated event is evaluated. These damages are then quantified in the third stage to estimate the resulting seismic losses. Finally, the SLCC of the pipeline is determined by aggregating the costs associated with all simulated events. This section has outlined the four main stages of the proposed methodology. Given the significant role of uncertainty in this approach, the next section presents probabilistic models to account for these uncertainties at each stage of the framework. Ultimately, the methodology is refined and structured through Monte Carlo simulation. Further details of each stage of the proposed framework are provided in the following sections, while the key formulas for each stage are summarized in Table 1. For more comprehensive explanations and detailed derivations, the reader is referred to the work of Alavi and Mashayekhi [29].

2.1 Seismic scenario hazard simulation

The first and fundamental step of the proposed framework involves seismic hazard analysis. Various methods are available for assessing seismic hazard, including both deterministic and probabilistic approaches [41]. While deterministic methods consider only a single worst-case earthquake, probabilistic approaches capture the full spectrum of possible events, including those that may be less tangible [42]. In this study, a stochastic scenario-based method is used for the potential occurrence of seismic hazards. As mentioned earlier, stochastic scenario-based approaches offer a practical solution by defining realistic earthquake events, allowing detailed simulation of ground motions and their effects. The generation of different scenarios is typically based on the characteristics of regional seismic sources, which are identified using historical and geological data [43]. For the generated scenarios, dominant magnitude–distance pairs are extracted to completely define the parameters of each scenario, including magnitude, location, rupture characteristics, and other relevant details, using the probabilistic model presented later in this paper.

Once all scenario parameters are established, ground motions at various sites are simulated using ground motion prediction equations (GMPEs) to obtain the corresponding seismic intensity measures. Based on these estimated seismic intensity measures, the potential occurrence of TGD and PGD hazards along the pipeline is subsequently evaluated, as detailed in the following sections.

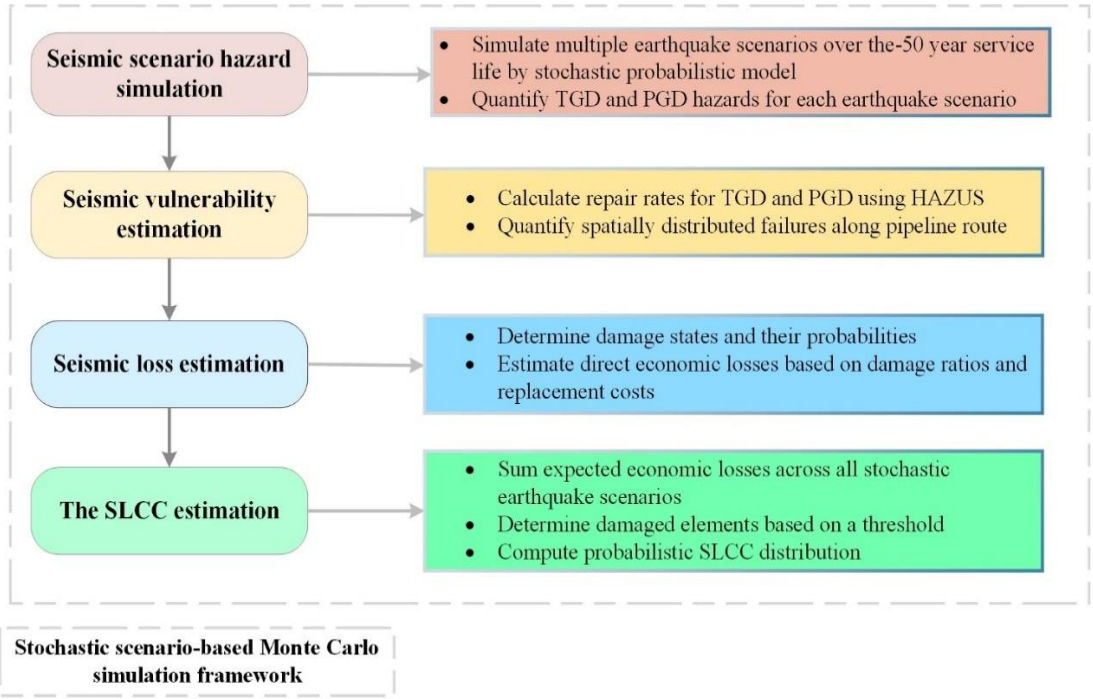


Fig. 1: Flowchart of the proposed stochastic scenario-based Monte Carlo framework for SLCC estimation of buried pipelines

During earthquakes, TGD hazard can impose significant stress and strain on buried pipelines. Peak ground velocity (PGV) is generally considered a more suitable measure than peak ground acceleration (PGA) for evaluating pipeline response, largely due to the confining effect of the surrounding soil [44]. However, conventional methods for estimating PGV, such as acceleration integration, ground motion prediction equations, or response spectrum analysis, are often affected by uncertainties related to soil variability and limited data [45]. To overcome these limitations, empirical PGV models such as those implemented in HAZUS [40] provide a practical means for assessing TGD hazards in buried pipelines, as shown in Equation (1). Unlike TGD hazards, which may affect a broad area but generally result in moderate impacts, PGD hazards typically occur over localized regions [44]. They can cause severe and concentrated damage to pipelines, with their manifestation strongly dependent on local site conditions.

To quantify PGD hazards, empirical models recommended by HAZUS [40] are employed. During seismic events, ground shaking increases pore water pressure in saturated soils, which reduces their shear strength and causes them to behave like a fluid [46].

This process generates fluctuating stresses that can destabilize buried pipelines, influenced by soil type and condition. The HAZUS [40] utilizes a soil liquefaction susceptibility map, which categorizes susceptibility into several levels, to estimate the probability of liquefaction based on groundwater depth and moment magnitude (Equation (2)) [47]. Using the formulas provided in HAZUS [40], the corresponding PGD displacement resulting from liquefaction can subsequently be derived. For further details, the reader is referred to [40]. Similarly, earthquake-induced landslides occur when seismic shaking reduces slope stability, especially on steep or unconsolidated terrain. Critical acceleration, which represents a slope's resistance to failure under dynamic loading, is used to assess landslide susceptibility. Geological features, groundwater conditions, and slope inclination are incorporated to develop detailed landslide susceptibility maps. Using these maps, PGD from landslides is quantified, providing spatially explicit estimates of PGD hazard potential along the pipeline route, as expressed in Equation (3) [40].

2.2 Seismic vulnerability estimation

After simulating seismic hazards, the next step in the proposed framework is to assess the seismic vulnerability of the buried pipeline. Seismic vulnerability describes the relationship between the intensity of earthquake-induced hazards and the resulting level of damage in the pipeline. In this study, pipeline vulnerability is assessed considering both TGD and PGD, with seismic damage typically quantified using the R_R to reflect event severity. As a vulnerability metric, R_R offers a practical measure of pipeline damage and allows quantification of spatially distributed failures. While R_R captures overall vulnerability, defining damage states provides a more detailed understanding of specific damage mechanisms.

Table 1: Summary of key equations employed in the proposed SLCC estimation framework for buried pipelines [29]

Equation. No.	Formula	Description
(1)	$PGV = \left(\frac{386.4 * S_{a1}}{2\pi}\right) \Big/ 1.65$	TGD hazard estimation
(2)	$P[Liquefaction] = \frac{P[Liquefaction \mid PGA = pga]}{K_M . K_W} * P_{ml}$	Liquefaction probability
(3)	$E[PGD] = E[\frac{d}{a_{is}}] * a_{is} * n$	PGD from landslides
(4)	$R_{R-TGD} = 3.1623 * PGV^{2.25}$	R_R for TGD
(5)	$R_{R-PGD} = 1.6052 * PGD^{0.319}$	R_R for PGD
(6)	$P_f = 1 - e^{(-RR*L)}$	Poisson failure probability
(7)	$P_{comb}[ds > DS2] = 1 - [(1 - P_{TGD}[ds \geq DS2]).(1 - P_{PGD}[ds \geq DS2])]$	Combined probability of a break
(8)	$P_{comb}[ds > DS1] = 1 - [(1 - P_{TGD}[ds \geq DS1]).(1 - P_{PGD}[ds \geq DS1])]$ $P_{comb}[ds = DS2] = P_{comb}[ds \geq DS2], P_{comb}[ds = DS1] = P_{comb}[ds \geq DS1] - P_{comb}[ds \geq DS2]$	Combined probability of leak Expected damage states probability
(9)	$EL_n = DR_C \times RV$ $DR_C = \sum_{i=1}^{N_{DS}} \sum_{k=1}^{k=n} (DR_i \times P_{comb}[ds = DSi]_k)$	Economic loss and compounded damage ratio
(10)	$C_{SLCC} = \sum_{m=1}^{Scenario} \sum_{p=1}^{event} EL$	SLCC estimation

S_{a1}: spectral acceleration in period 1-second, K_M and K_W: correction factor of moment magnitude and groundwater level, P_{ml}: the percentage of the mapped area that can liquefy, $P_{comb}[ds \geq Dsi]$: is the joint exceedance probability, DR_C: is the compounded damage ratio, N_{DS}: the total number of considered damage states.

Damage states for buried pipelines are commonly defined based on physical response indicators, such as axial and bending strain demands, joint deformation, leakage occurrence, or loss of structural integrity [22]. In this study, the damage state classification follows HAZUS [40], which defines two primary damage states: leakage and breakage based on the strain demand developed in the pipeline. Although other intermediate damage conditions may occur, only those leading to leakage or breakage are considered, as they directly affect pipeline functionality and contribute to seismic losses. Following this framework, the two HAZUS-recommended damage states are incorporated using empirical R_R relationships, as shown in Equations (4) and (5) [48, 49]. Although the adopted R_R model is based on HAZUS-recommended empirical relationships, its application is considered appropriate for this study. This is because the key characteristics governing the seismic response of buried steel transmission pipelines, including welded joints, burial depth, soil–pipe interaction, and geometric properties, are generally consistent across different regions [6]. Moreover, HAZUS-based RR formulations have been widely applied worldwide and have shown satisfactory performance for pipeline systems with characteristics comparable to those of the studied Iranian gas pipeline [6, 29, 50, 51]. Therefore, despite being calibrated using international case histories, these empirical relationships can be reasonably applied to the present case as first-order approximations within the probabilistic SLCC framework. Damage from TGD is mainly manifested as compressive stress at pipeline joints, predominantly causing leakage, whereas PGD-induced damage is more likely to result in structural breakage. Accordingly, for TGD hazards, roughly 80% of damage is attributed to leakage and 20% to breakage, with the reverse assumed for PGD hazards [40]. These proportions are adopted to realistically represent the dominant failure mechanisms associated with each type of seismic hazard.

2.3 Seismic loss estimation

Seismic loss estimation is the subsequent step after hazard simulation and vulnerability assessment, translating earthquake-induced damage into quantifiable economic impacts. In this study, the economic consequences of earthquake-induced pipeline damage are quantified primarily in terms of direct repair and replacement costs, representing the immediate expenditures required to restore damaged pipeline segments. Such costs are commonly used in seismic risk assessments of buried pipelines. Indirect consequences, including service interruption losses and broader social or environmental impacts, are not explicitly included in the present cost model, as their quantification requires detailed information on network operation, restoration processes, and regional economic interactions that are beyond the scope of this component-level analysis.

In this stage, the damage states and R_R obtained from the vulnerability analysis are used to estimate the expected losses for each seismic scenario. The expected number of pipeline failures associated with each damage state is estimated by combining the failure probability of individual pipeline segments with their corresponding lengths. The probability of failure for the pipeline (P_f) is evaluated using a Poisson-based formulation, as expressed in Equation (6). This probabilistic representation allows discrete failure occurrences to be consistently modeled over continuous pipeline segments. To account for TGD and PGD hazards, the exceedance probabilities associated with the two damage states are jointly considered. Under the assumption that damages induced by TGD and PGD hazards are statistically independent, their combined exceedance probabilities are computed using Equation (7) [51]. This approach enables the simultaneous consideration of multiple hazard sources while maintaining computational efficiency and avoiding the need to explicitly model complex interactions between different damage mechanisms [29]. The occurrence probabilities of the expected damage states are evaluated using Equation (8), forming a key input to the seismic loss estimation process. Quantifying pipeline damage in economic terms is essential for supporting informed decision-making. Each damage state represents a specific pipeline performance level with distinct functional and economic impacts. Linking seismic demand to these states allows physical damage to be consistently translated into expected losses. At this stage, seismic losses are quantified by integrating the probabilistic characterization of pipeline damage with corresponding economic consequences. The estimation of direct economic losses for gas pipelines requires consideration of spatial pipeline characteristics, seismic demand levels, and repair or replacement costs associated with different damage severities [52]. Following HAZUS [40], the loss assessment focuses on leakage and breakage. Direct economic loss is therefore calculated by weighting the replacement value of the pipeline with damage-specific cost ratios and the combined probabilities of the associated damage states. This formulation provides a consistent probabilistic link between seismic damage occurrence and expected economic impact, as expressed in Equation (9) [53]. Damage severity is incorporated through damage ratios, representing the proportion of pipeline replacement value associated with each damage state. These ratios, reported in [53], quantify the relative economic impact of different damage levels for buried pipelines, with replacement costs normalized to $1,000 per unit length. A constant replacement value is assumed for both damage states, while differences in economic impact are captured through the assigned damage ratios.

2.4 The SLCC estimation

The SLCC estimation extends the analysis of pipeline damage and losses by integrating the probabilistic impacts of multiple seismic events over the entire service life of the system. Unlike single-event loss assessments, SLCC accounts for the cumulative economic consequences of multiple seismic scenarios, providing a comprehensive measure of long-term risk exposure [54]. In this framework, seismic scenarios generated in the hazard analysis phase are explicitly considered in the SLCC computation. Each scenario is characterized by its magnitude, location, and ground motion parameters, along with an associated occurrence probability. Pipeline damage is quantified using R_R (Equations (4) and (5)) for leakage and breakage states.

To appropriately represent the typical characteristics of seismic damage in pipelines, the occurrence of pipeline failures is modeled as a Poisson process, as expressed in Equation (6). This approach is suitable because failures occur as discrete events, are relatively rare over long transmission segments, and, given the local seismic demand, can reasonably be considered independent of one another [55]. Once the pipeline damage states are identified, the expected probability of each damage state is first obtained by integrating the multi-hazard effects according to Equation (7). In estimating the overall damage probability, the contributions associated with TGD and PGD are combined, assuming no statistical dependence between the two mechanisms. Although both processes are driven by the same earthquake and may be influenced by related intensity measures, reliable empirical information describing their joint behavior is currently limited. In the absence of a well-established model for their correlation, treating the two effects separately provides a practical approximation consistent with common practice in seismic risk assessments of buried pipelines. It is recognized that some level of correlation may exist because both mechanisms are linked to the characteristics of the causative earthquake. Consequently, the calculated combined damage probability should be interpreted with this modeling simplification in

mind, although its influence is expected to remain within the broader uncertainty associated with the R_R and hazard representation adopted in this study.

Subsequently, the discrete damage probabilities are estimated using Equation (8) to quantify the seismic damage along the pipeline. Finally, the cost associated with seismic damage to the pipeline is calculated using Equation (9). These scenario-specific losses are then weighted by the probability of occurrence, providing the expected cost contribution of each event. The SLCC is obtained by aggregating the expected losses of all scenarios over the pipeline's service life, accounting for the temporal distribution of earthquake occurrences, as expressed in Equation (10). This probabilistic, scenario-based approach ensures that both frequent low-intensity and rare high-intensity events are properly represented in the economic assessment, resulting in a robust and comprehensive estimation of SLCC.

3. Probabilistic model

This section begins with an introduction to probabilistic modeling, which plays a central role in capturing uncertainties throughout the SLCC assessment conducted in this study. At each stage of the process, various sources of uncertainty must be represented as random variables in the model inputs. Each realization of these variables produces corresponding economic costs in terms of seismic loss, which in turn contribute to the overall SLCC estimation. Earlier studies have demonstrated the effectiveness of this approach. Rahimi and Mahsuli [56] employed random variables to perform hazard analysis for a specific region, while Hosseini and Karami Mohammadi [57] examined seismic resilience of urban transportation networks using an uncertainty-based framework.

$$f_m(m) = \frac{b * e^{(-b*(m-M_{\min}))}}{1-e^{(-b*(M_{\max}-M_{\min}))}} \quad (11)$$

Based on these concepts, this section provides a comprehensive description of the probabilistic models employed in the proposed methodology. The treatment of uncertainties begins at the earliest stage of the framework, namely the seismic hazard analysis, and systematically propagates through all subsequent steps up to the estimation of economic losses and SLCC. The incorporation of random variables at each stage of the process is described in detail in the following sections.

3.1 Seismic hazard uncertainty

In earthquake engineering, seismic sources are a fundamental concept used to characterize potential earthquake activity within a region. In area-based models, these sources are typically defined based on the spatial distribution of past earthquakes, as well as the correlation of fault mechanisms with observed seismicity [50]. Since seismic sources are constructed from seismological data, they can be characterized by parameters such as occurrence rate, maximum and minimum moment magnitude (M_{max} and M_{min}), and source location [43]. Each of these parameters inherently carries uncertainty due to limitations in historical records, measurement errors, and natural variability in tectonic processes [58]. On the other hand, GMPEs are derived from available observational data using statistical analyses, and they inherently contain uncertainties. The probabilistic models considered in the seismic hazard analysis, which ultimately generate a specific earthquake scenario for a given source, are presented in the following.

3.1.1 Occurrence model

For each seismic source, an occurrence model simulates the random timing of seismic events within that source. A commonly used approach for this purpose is the Poisson distribution process [59]. This choice reflects the discrete and relatively rare nature of earthquake occurrences over a specified time interval, assuming a stationary occurrence rate for each source. The model requires as input the event occurrence rate and the time period of interest, denoted by λ and T, respectively, as illustrated in Figure 2. In this study, uncertainties in the occurrence rates are explicitly addressed by treating them as random variables, allowing the model to capture the natural variability in seismic activity. With each sampling of the occurrence rate model, the number of earthquakes that may occur within the specified time period for a given seismic source is determined. Subsequently, the characteristics of each event, such as magnitude, location, and other relevant parameters, must be specified to fully define the earthquake scenario.

3.1.2 Magnitude model

In the probabilistic models, earthquake moment magnitude is treated as a fundamental random variable governing seismic demand and subsequent damage and loss estimates. For each seismic source, earthquake magnitudes are generated using a truncated Gutenberg–Richter magnitude–frequency relationship [60], which is widely adopted in probabilistic seismic hazard analysis due to its ability to represent the observed exponential decay of earthquake frequency with increasing magnitude while enforcing physically meaningful bounds. Specifically, earthquake magnitudes are sampled from a bounded exponential distribution bounded by M_{min}, representing the smallest event capable of causing engineering-relevant effects, and M_{max}, which reflects the largest seismic potential of each source. The corresponding probability density function is given by Equation (11) [41].

This formulation remains consistent with the regional seismicity characteristics while simultaneously bounding earthquake magnitudes within physically meaningful ranges, thereby preventing the occurrence of unrealistically large events. Equation (11) provides the probability of occurrence for a specific moment magnitude value. However, in the proposed model of this study, the goal is to generate a physical response quantity rather than merely a probability [41]. To achieve this, random earthquake moment magnitudes are generated using inverse transform sampling based on the Gutenberg–Richter relationship, while treating M_{max}, b, and U as random variables, as expressed in Equation (12).

$$M = M_{\min} - \frac{1}{b}\ln[1-U(1-e^{-b*(M_{\max}-M_{\min})})] \quad (12)$$

where U is a uniformly distributed random variable in the interval [0,1].

3.1.3 Location model

For area seismic sources, the earthquake hypocenter location is commonly modeled assuming a uniform spatial distribution of seismicity within the boundaries of the source polygon [61]. This approach reflects the lack of sufficient geological or geophysical evidence to define specific fault traces or preferential rupture locations within the zone. Consequently, every point within the polygon is considered equally probable for earthquake nucleation. In this study, hypocenters are sampled using a Monte Carlo approach, whereby random points are generated within the polygonal boundary and accepted only if they lie inside the defined geometry, ensuring accurate representation of the source area.

The source-to-site distance for each simulated event is then calculated directly from the randomly sampled hypocenter to the site of interest. This method inherently captures aleatory variability in earthquake location, while introducing no additional epistemic uncertainty beyond the delineated polygonal boundaries. This approach is consistent with standard practices in probabilistic seismic hazard analysis for regions with diffuse or background seismicity, as recommended in widely used frameworks such as the USGS National Seismic Hazard Model. While the rejection sampling method used here is straightforward and widely adopted, alternative approaches such as triangulation-based sampling or grid-based sampling can also be employed for polygons with complex geometry, offering faster computation and controlled spatial resolution of hypocentral points.

3.1.4 GMPEs model

The GMPEs, also known as attenuation relationships, are statistical models used to estimate earthquake ground motion intensity measures as functions of earthquake magnitude, source-to-site distance, faulting mechanism, and local site conditions [41]. These equations are developed through regression analysis of extensive strong-motion databases obtained from recorded earthquakes and are formulated to capture the combined effects of source, path, and site characteristics [62]. The regression structure typically incorporates model coefficients that represent the contributions of these parameters, together with residual terms that describe ground-motion variability. The total variability is conventionally decomposed into inter-event and intra-event components, representing event-to-event differences and spatial variability of motions within a single event. In this study, the regression coefficients as well as the inter-event and intra-event residuals are treated as random variables to explicitly account for uncertainty in ground motion prediction and enable a realistic propagation of uncertainty from seismic sources to site-specific intensity measures through the subsequent SLCC analyses. To address epistemic uncertainty in ground-motion modeling, a stochastic weighting scheme is employed to combine multiple GMPEs. Let IM_i denote the intensity measure predicted by the i-th GMPE, and let w_i be its corresponding weight. The combined estimate is obtained by Equation (13).

$$IM = \sum_{i=1}^{N} w_i IM_i \quad (13)$$

which represents a weighted linear combination of the individual GMPE predictions. The weights are constrained to ensure a valid probabilistic mixture, such that $\sum_{i=1}^{N} w_i = 1, w_i \geq 0$. In the case of the three GMPEs considered in this study, the weights are generated through a sequential sampling scheme to satisfy these constraints. The first two weights are sampled from uniform distributions. $w_1 \sim \mathrm{U}(0,1)$, $w_2 \sim \mathrm{U}(0,1-w_1)$, and the third weight is assigned as $w_3 = 1 - w_1 - w_2$. The probability of selecting GMPE i during random sampling is defined by Equation (14):

$$w_i = P(GMPE_i) \quad (14)$$

This formulation ensures that all weights remain non-negative and that their sum equals one, thereby eliminating the possibility of invalid or negative weight combinations. The stochastic weighting scheme provides a transparent and reproducible representation of epistemic uncertainty across the GMPE ensemble and can be readily extended to larger model sets using the same sequential sampling strategy.

3.2 Seismic vulnerability uncertainty

Buried pipelines are often challenging to observe directly due to security concerns and the difficulty of post-earthquake inspections, resulting in limited available data. Consequently, the seismic vulnerability of pipelines in this study is assessed using R_R relationships, which are derived from empirical observations and correlations with varying intensities of strong ground motions. Given their empirical nature, these relationships inherently involve a degree of uncertainty. Following the approach proposed by Alavi and Mashayekhi [29], pipeline repair demand is therefore treated as a random variable, and the R_R functions are modeled using a probabilistic distribution, where the mean value corresponds to the estimated seismic hazard in each pipeline segment. Moreover, this approach allows the incorporation of variability arising from differences in soil conditions, pipeline materials, and installation practices, while being directly integrated into segment-based SLCC assessments to reflect realistic post-earthquake repair demands.

In the proposed SLCC framework, the residual epistemic uncertainty associated with the empirical R_R models is explicitly represented by model parameters treated as random variables. This allows the variability in pipeline vulnerability, arising from possible deviations between the empirical relationships and the actual behavior of the case study, to be propagated through the SLCC analysis.

3.3 Monte Carlo simulation framework for SLCC assessment

Each seismic source is modeled as an independent earthquake-generating entity. Using a Monte Carlo simulation approach, all relevant random variables are considered to explore the range of possible earthquake scenarios. For each source, the number of earthquake events over a 50-year service life is drawn from a Poisson distribution based on a sampled occurrence rate. For each scenario, earthquake magnitudes are sampled from the source-specific magnitude model, and hypocentral locations are randomly assigned according to the location model. Ground motion intensity at the site is then computed using GMPEs, with the coefficients implemented as random variables to capture aleatory uncertainty. The resulting site-specific intensity values are used to assess potential hazards, such as TGD and PGD, at the site. Based on the estimated TGD and PGD hazards, R_R are derived probabilistically using damage functions tailored to the site. Event-specific losses are subsequently calculated by combining the probabilities of different damage states with their corresponding economic consequences. The SLCC for the site is obtained by aggregating losses across all simulated scenarios. This step-by-step Monte Carlo approach provides a probabilistic assessment of SLCC by capturing key sources of uncertainty over the pipeline's service life. The random variables employed in the probabilistic models and Monte Carlo simulation, as illustrated in Figure 2, are provided with full details in Table 2. In this procedure, the statistical distributions of the random variables are adopted in accordance with the formulations and assumptions presented in the studies by Rahimi and Mahsuli [56] and Alavi and Mashayekhi [29].

4. Case study

This section evaluates the proposed framework through a case study. Because the main goal of this study is to estimate the SLCC of a buried pipeline, a pipeline in a seismically active region is chosen to provide a more realistic and informative evaluation of the proposed method. The following subsections describe the study area and pipeline details relevant to each step of the framework.

4.1 Overview of the studied region and gas pipeline

Fars Province, situated in southwestern Iran between approximately 27°–31° N latitude and 50°–55° E longitude, forms part of the Zagros Fold and Thrust Belt, one of the most seismically active regions in the Middle East. The area's tectonic activity arises from the ongoing collision between the Arabian and Eurasian plates, a major continental convergence that has shaped the Iranian Plateau and continues to generate frequent seismic events [63].

Within Fars, this interaction produces complex and diffuse seismicity, marked by numerous active faults. The gas transmission pipeline under study is located in this seismically active region, stretching across Fars Province and passing through Shiraz, the provincial capital. Along its pipeline route, it crosses a variety of geomorphological and environmental landscapes, as shown in Figure 3.

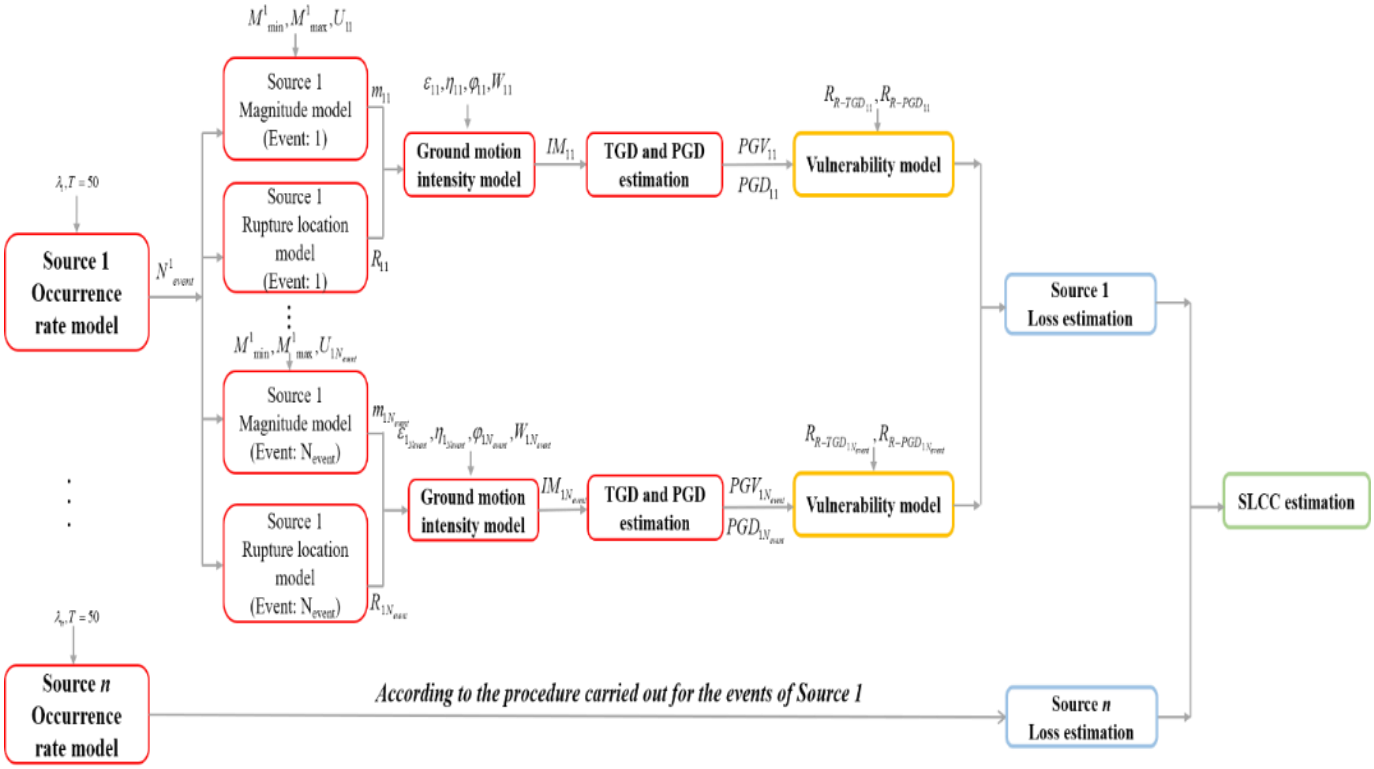


Fig. 2: Uncertainty propagation in stochastic scenario-based SLCC estimation

Table 2: Random variables and uncertainty modeling in SLCC estimation

Symbol	Description	Parameter type	Characteristics
λ_i	Annual occurrence rate of source *i*	Random variable	Lognormal
b_i	Magnitude distribution parameters for seismic source *i*	Random variable	Lognormal
T	Service life	Constant	50
R_i	Distance from the rupture location to the site	Random variable	Uniform
M_{min}	Minimum magnitude	Constant	4.5
m_i	Magnitude of source *i*	Model response	-
IM	Intensity measure	Model response	-
ε_i	Intra-event ground motion prediction model error	Random variable	Normal (0,1)
η_i	Inter-event ground motion prediction model error	Random variable	Normal (0,1)
Φ_i	Vector of ground motion model regression coefficients	Random variable	Normal (0,1)
W_i	Vector of weight coefficients of each GMPE	Random variable	Normal (0,1)
$R_{R\text{-}TGD}$	R_R due to TGD hazard	Random variable	Lognormal (mean, 0.25)*
$R_{R\text{-}PGD}$	R_R due to PGD hazard	Random variable	Lognormal (mean, 0.25)*

* The mean value corresponds to the value computed based on the seismic intensity, as given by Equations (4) and (5).

However, due to the lack of publicly available information on key pipeline properties such as material, diameter, joint type, and burial depth, these parameters could not be directly incorporated into the analysis. Therefore, the HAZUS pipeline classification framework is adopted based on the limited available data. Although HAZUS assigns ductile pipelines a vulnerability reduction of about 70% compared to brittle ones, this factor is not applied in this study. Instead, the pipeline is conservatively modeled as a low-ductility system to avoid underestimating potential seismic damage and to account for uncertainties associated with insufficient pipeline specifications.

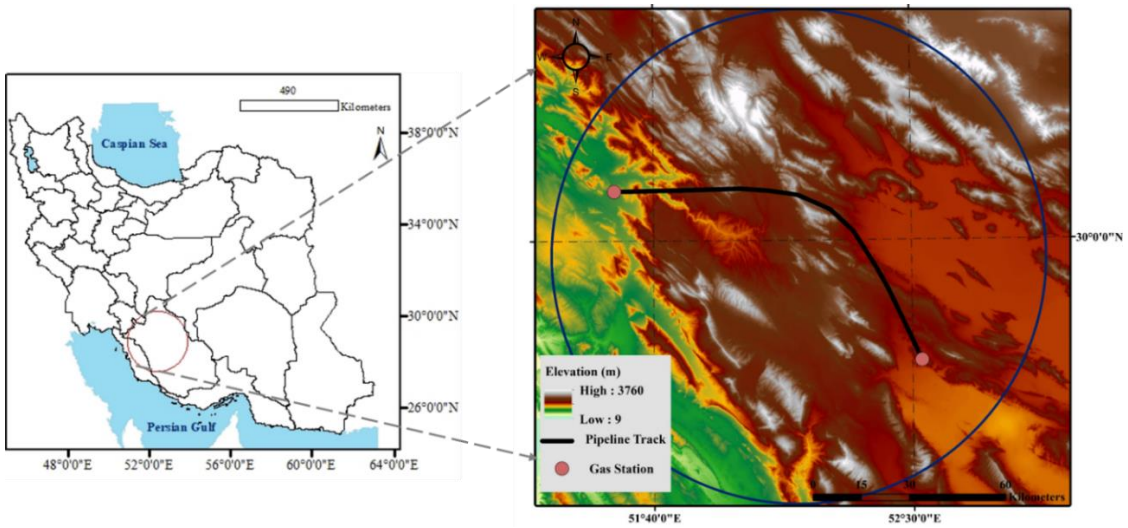


Fig. 3: Description of the study area and gas pipeline

On the other hand, Shiraz serves as a cultural, economic, and medical hub in southern Iran, with a population exceeding 1.8 million, placing it among the country's largest urban centers. Rapid urbanization and industrial expansion in recent decades have significantly increased energy demand, particularly for natural gas, to sustain residential and industrial growth. The pipeline is a key part of the regional gas network, built to maintain energy reliability despite challenging seismic and geological conditions. Due to Fars Province's seismotectonic complexity, its safe operation requires close attention to geological, geotechnical, and seismic factors along the route.

4.2 Region seismicity and secondary hazards

Fars Province is highly seismically active, located within the Zagros Fold and Thrust Belt, where ongoing plate convergence causes frequent crustal deformation. Historical and instrumental records indicate numerous moderate to strong earthquakes, typically between Mw 4.0 and 6.7, including the 1972 Qir earthquake (Mw 6.7) and the 1993 Firuzabad earthquake (Mw 5.4). Seismic activity is distributed across multiple faults rather than a single fault [63]. This seismicity highlights the ongoing tectonic activity and provides essential information for assessing hazard and potential impacts on critical infrastructure, such as the studied gas pipeline.

The first step in characterizing the seismic sources in the study area is the compilation of a reliable and comprehensive earthquake catalog. In this study, instrumental seismic data provided by the International Institute of Earthquake Engineering and Seismology (IIEES) [64], covering the period from 1926 to 2020, are used. As illustrated in Figure 4, the seismic sources are modeled as area sources. Moment magnitudes in the catalog are homogenized, and dependent events such as foreshocks and aftershocks are removed using standard decluttering procedures. Seismicity parameters for each area source are estimated using the Gutenberg–Richter relationship [60] in conjunction with a Poissonian occurrence model. Given that seismic activity in Fars Province is spatially distributed across multiple structures rather than confined to a single mapped fault, an area-source representation is considered appropriate. Based on the spatial distribution of earthquakes in the processed catalog, several seismic source zones are therefore defined within the study area, as shown in Figure 4.

The resulting probabilistic seismic hazard parameters, including the M_{max}, are summarized in Table 3, with mean values informed by regional studies such as Alavi et al. [5, 52]. In this study, M_{max} for each source is estimated using a widely adopted and internally consistent approach. First, the largest observed moment magnitude within each source zone was identified from the instrumental catalog. Then, an additional 0.5 magnitude unit was added to account for epistemic uncertainty. This criterion is applied uniformly to all area sources and leads to M_{max} values that are tectonically reasonable for the Zagros Fold and Thrust Belt. While the estimated M_{max} values may show minor differences compared with those reported in previous studies (e.g., Mahsuli et al. [65]), they remain within a comparable and physically consistent range for the regional seismicity. Such differences mainly reflect variations in the delineation of seismic source zones among studies, rather than fundamental discrepancies in the underlying seismic potential. The *b*-parameter listed in Table 3 characterizes the slope of the Gutenberg–Richter frequency–magnitude distribution and controls the relative proportion of small and large earthquakes within each seismic source.

After characterizing the seismic sources and their occurrence models, the ground motion at the site is estimated using GMPEs, which relate ground-motion intensity to

earthquake magnitude, source-to-site distance, and site conditions.

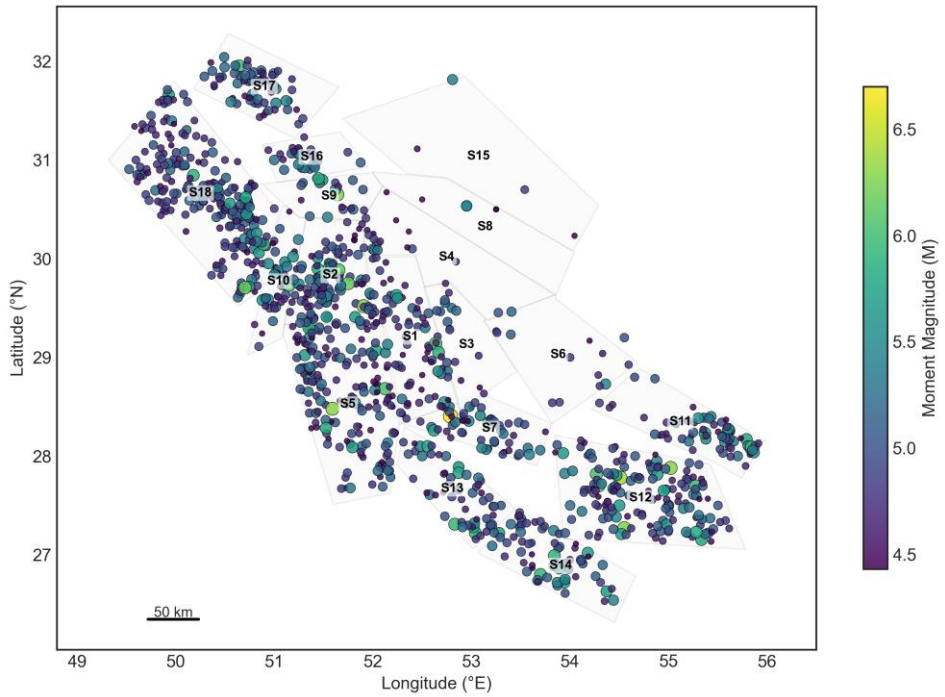


Fig. 4: The case study seismic detail with the distribution of the earthquake and seismic source model

Table 3: Seismicity parameters for the 18 area sources considered in the analysis

Source	λ (per year)		b		M_{max}	
	Mean	SD	Mean	SD	Mean	SD
1	0.396	0.1	1.007	0.15	6.34	0.15
2	0.564	0.1	0.77	0.15	6.4	0.15
3	0.074	0.1	0.992	0.15	5.33	0.15
4	0.091	0.1	0.803	0.15	5.5	0.15
5	0.806	0.1	1.007	0.15	6.48	0.15
6	0.059	0.1	0.903	0.15	5.74	0.15
7	0.298	0.1	0.906	0.15	8.8	0.15
8	0.016	0.1	0.477	0.15	6.3	0.15
9	0.125	0.1	0.665	0.15	6.74	0.15
10	0.226	0.1	0.797	0.15	6.19	0.15
11	0.361	0.1	0.778	0.15	6.3	0.15
12	0.85	0.1	0.772	0.15	6.51	0.15
13	0.324	0.1	0.608	0.15	6.05	0.15
14	0.383	0.1	0.633	0.15	6.02	0.15
15	0.03	0.1	0.524	0.15	5.9	0.15
16	0.142	0.1	0.566	0.15	5.51	0.15
17	0.312	0.1	1.073	0.15	6.25	0.15
18	0.218	0.1	0.781	0.15	7.7	0.15

In this study, three GMPEs are employed, namely those proposed by Akkar and Bommer [66], Akkar et al. [67], and Cornel et al. [68]. The first two GMPEs are developed as part of the EMME project [69], specifically tailored for the Middle East region, making them particularly suitable for our study area. Conversely, the formulation by Cornel et al.

[68] serves as a more general alternative and is included to provide a simplified perspective. In this study, all GMPEs are integrated using randomly assigned weighting factors to account for epistemic uncertainty. The inclusion of the Cornel et al. [68] GMPE offers a computationally efficient way to capture the broad variability of seismic hazard while maintaining a level of simplicity, thereby acting as a practical benchmark alongside the region-specific models. While the selected GMPEs effectively represent the variability of ground-motion intensity measures associated with seismic sources, earthquake-induced hazards are not limited to TGD effects alone. Notably, PGD resulting from local geotechnical conditions can significantly impact pipeline performance and thus requires explicit consideration. Figure 5 presents the susceptibility of the pipeline route to soil liquefaction and landslides. Figure 5a is based on the liquefaction hazard map prepared by the International Institute of Earthquake Engineering and Seismology, whereas Figure 5b uses the landslide susceptibility map developed by the Geological Survey of Iran. These maps integrate both geotechnical and seismic parameters and provide the basis for PGD hazard assessment following the HAZUS framework [40]. Figure 5a indicates that 42% of the route lies in non-susceptible areas, 48% in low susceptibility zones, and 10% in moderate zones, with no segments in high susceptibility areas. Figure 5b shows the pipeline crossing landslide susceptibility zones V, VII, X, and XII in roughly equal proportions.

After identifying the seismic sources and assessing the pipeline's sensitivity to PGD hazards along its route, the proposed methodology proceeds by generating different earthquake scenarios over the 50-year service life of the pipeline, based on the characteristics of the probabilistic model described in the previous section. For each specified scenario, all steps are illustrated in Figure 1, which outlines the general procedure for estimating the SLCC, and are implemented. Further details on this process are provided in the following sections. Given the considerable length of the studied gas pipeline and its passage through diverse regions, the analytical framework employed in this study is elaborated in the subsequent section.

4.3 Segment-based analysis of the studied pipeline

The studied gas pipeline crosses regions with diverse seismic and geological conditions, which can cause variations in its response during earthquakes. To capture these differences and improve the accuracy of seismic risk assessments, the pipeline is divided into 1,000-meter segments, with each segment's midpoint representing local conditions for analyses such as seismic hazard evaluation and physical vulnerability assessment [6]. A segment length of 1,000 meters is selected to match the spatial resolution of input datasets such as topography, land use, and hazard layers, which typically range from 30 m to several hundred meters. Smaller segments would add computational cost without improving accuracy, while larger ones could obscure local variations and underestimate high-risk areas. This selection is consistent with the data-granularity considerations discussed by Alavi et al. [52]. Alternative approaches, such as treating the pipeline as a single uniform system or dividing it into much larger sections, may overlook local variations in soil properties, topography, or seismic intensity. While simpler, these methods can lead to under- or overestimation of hazard and damage in specific areas, reducing the reliability of SLCC estimates [29]. By contrast, the segment-based approach allows hazard and vulnerability parameters to be applied individually to each segment, reflecting the spatial variability of local conditions. This not only enhances the precision of the analysis but also facilitates aggregation of segment-level results to produce a comprehensive, spatially resolved estimate of the pipeline's SLCC. Thus, the proposed framework enables more realistic assessment of seismic performance and economic impacts for long, geographically diverse pipelines.

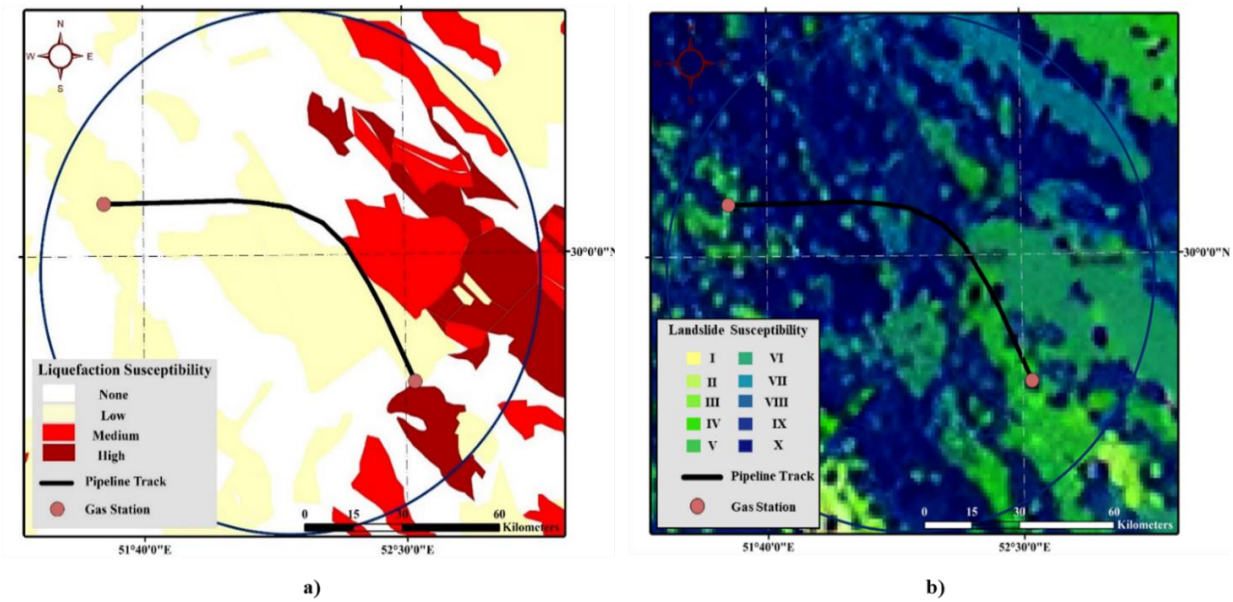
Using the approach adopted in this study, all steps of the SLCC calculation are applied to each pipeline segment individually. For each segment, seismic hazards are assessed, followed by estimation of segment-specific vulnerability. The resulting damage probabilities are then converted into economic losses, and the potential costs of all segments are aggregated to determine the loss for the entire pipeline in a specific earthquake scenario. Following the procedure outlined, the results are presented in the next section.

5. Results

After identifying the seismicity parameters of the study region, along with other factors influencing the estimation of SLCC, the proposed methodology employs a Monte Carlo simulation framework to evaluate the SLCC. In each simulation run, the seismic hazard parameters are sampled to account for inherent uncertainties in the analysis. Specifically, earthquake scenarios characterized by their locations and magnitudes are generated through random sampling from probabilistic seismic hazard models. To control computational complexity, 1,000 Monte Carlo simulations are conducted in this study. However, future research may adopt a larger number of simulations or convergence-based stopping criteria to improve estimate accuracy.

This section examines the distribution of the SLCC of the investigated pipeline under stochastic earthquake scenarios within its service life. By considering multiple seismic hazards and their probabilistic interactions, various damage states are identified, which are then quantified in terms of

economic losses, ultimately leading to the estimation of SLCC across all considered scenarios.



a) b)

Fig. 5: Spatial PGD susceptibility of the pipeline: a) liquefaction; b) landslide susceptibility

The resulting outcomes, with seismic effects from diverse sources as primary contributors to SLCC, are presented and discussed in the following. Figure 6 shows a stochastic realization of earthquake events in the study area over 50 years, illustrating the spatial distribution and magnitudes of earthquakes from different sources.

As a key outcome of this study, Figure 7 illustrates the frequency distribution of the total SLCC accumulated along the pipeline, derived from stochastic earthquake scenarios associated with different seismic sources over a 50-year service life. This representation provides insight into the variability of long-term economic consequences arising from seismic activity. The resulting cost distribution displays a clear asymmetry, with a long tail extending toward higher values. For the majority of simulated earthquake realizations, the estimated losses fall within a moderate range of roughly $2 million to $3 million. However, the distribution also indicates a meaningful probability of infrequent but high-impact events, in which the total SLCC increased considerably and can exceed $4 million.

Figure 7 provides an overall view of the total SLCC of the pipeline within the study area. However, it does not distinguish the relative contributions of individual seismic sources or reflect the associated variability. To complement the analysis of the total SLCC, the SLCC distributions attributable to each seismic source are therefore examined separately for all 18 identified hazard sources. This source-specific decomposition enables the identification of dominant hazard contributors, facilitates comparison of cost dispersion and skewness among different sources, and supports the prioritization of seismic sources for informed decision-making. Figure 8 shows the frequency distribution of SLCC values for each of the 18 seismic sources considered in the analysis. These distributions are derived from the Monte Carlo simulation results, allowing a more detailed examination of the cost behavior associated with individual sources. The results indicate substantial variability in the cost distributions among different seismic sources, with the SLCC associated with some sources being several times greater than that associated with sources with lower contributions. For instance, the SLCC attributed to Source 2 is more than six times greater than that of Source 4, highlighting the contrasting influence of different seismic sources on the overall seismic risk of the pipeline. It should be noted that, in Figure 7, the parameters of the lognormal distribution are estimated in logarithmic space, while the mean and standard deviation are subsequently calculated and reported in the original SLCC scale. In this figure, the solid red line corresponds to the Gaussian kernel density estimation (KDE), whereas the blue dashed line represents the fitted lognormal distribution

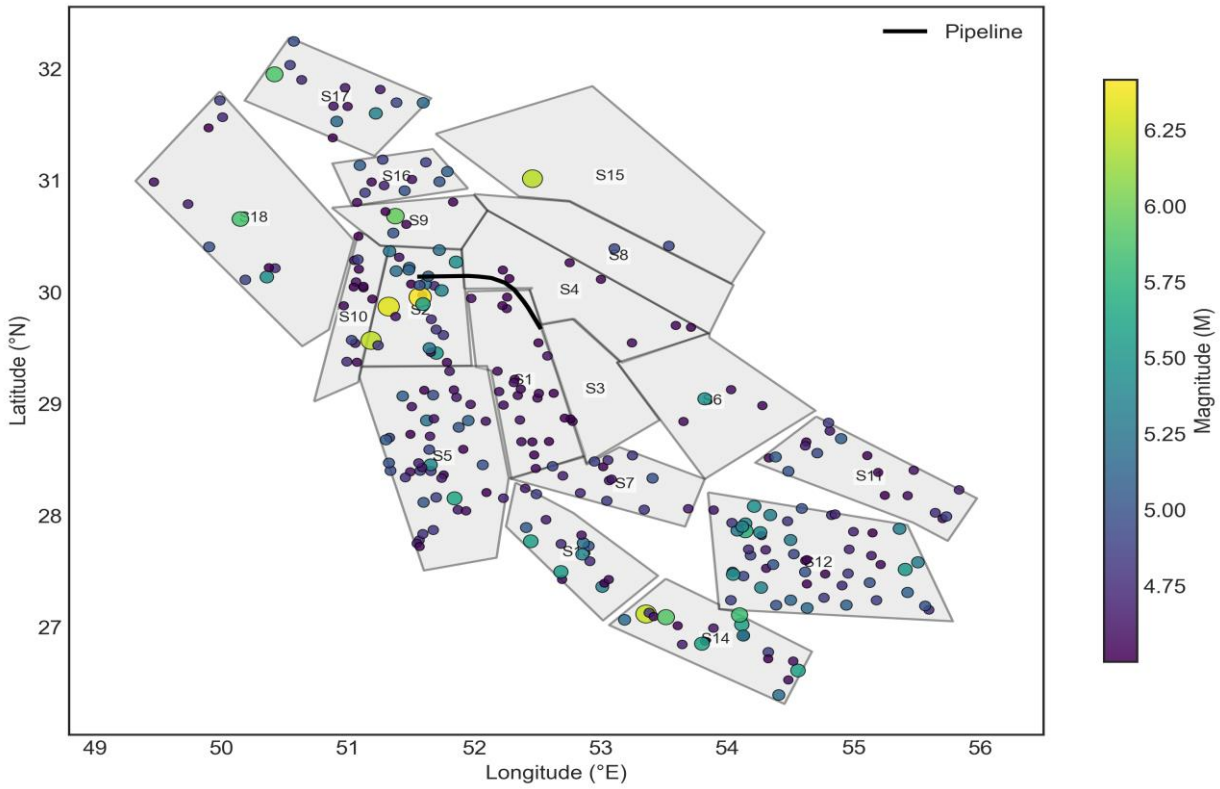


Fig. 6: One realization of the simulated earthquake occurrence distribution

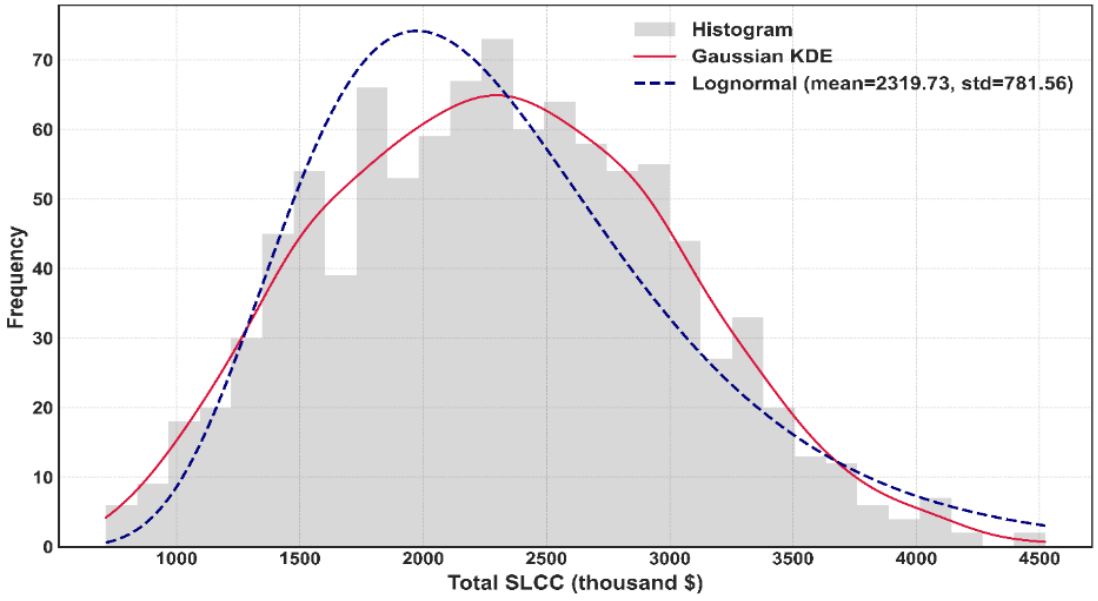


Fig. 7: Frequency distribution of the total SLCC of the buried pipeline

In the proposed methodology, the economic losses for each segment of the pipeline are estimated based on the probability of leakage and breakage damage states. These probabilities are obtained by combining the seismic demand produced by each seismic source with the corresponding R_R functions and the damage state models of the pipeline. Each seismic source contributes differently to the probability of the two damage states across the various pipeline segments. To account for this variability, the maximum probability of damage for each segment–source pair is evaluated over multiple simulation realizations, taking the larger of the leakage and breakage probabilities in each case. The average of these maximum probabilities is then used as a practical measure to estimate the relative contribution of each seismic source to potential damage along the pipeline.

This approach is appropriate because the mean of the maximum damage probabilities reflects both the most vulnerable pipeline segments and the seismic sources with the greatest influence on critical damage. In this way, it offers a clear and practical basis for prioritizing mitigation measures and for better understanding how the most significant risks from each seismic source are distributed along the pipeline. Figure 9 illustrates the mean of the maximum probabilities of damage occurring in different pipeline segments, attributable to each seismic source. Accordingly, identifying the contribution of each seismic source to the probability of these damage states is crucial for estimating the SLCC, as confirmed by the probabilities in Figure 9 and the corresponding SLCC values in Figure 8.

In the following, various details are presented. However, the analysis initially focuses on the most influential seismic sources that contribute the largest share to the total SLCC. These ten sources, which have the highest contributions, are shown in Figure 10, where the bars represent the average SLCC per source across all Monte Carlo realizations. Additionally, the contribution of each of these sources to the overall SLCC distribution is illustrated in Figure 11, which shows the percentage share of each source in the mean total SLCC. In this figure, the remaining seismic sources are grouped under the “Other sources” category, as each of them contributes only a minor share compared with the dominant sources.

Figure 12 highlights the 10 seismic sources with the highest average number of earthquake events over the study period. As shown, although Source 12 experienced a larger number of events, Figure 11 indicates that its contribution to the SLCC is relatively low. Conversely, Source 2, despite having fewer events, accounts for a larger share of the SLCC. This figure effectively emphasizes sources that are not only potentially destructive but also occur with higher frequency, providing insight into their relative contributions to the overall SLCC.

The exceedance probability curve is one of the key outputs of probabilistic seismic risk analysis, illustrating the relationship between the predicted SLCC and the probability of exceeding that value over a specified period. This curve is constructed by ranking the Monte Carlo simulation SLCC realizations in descending order and computing the empirical exceedance probability.

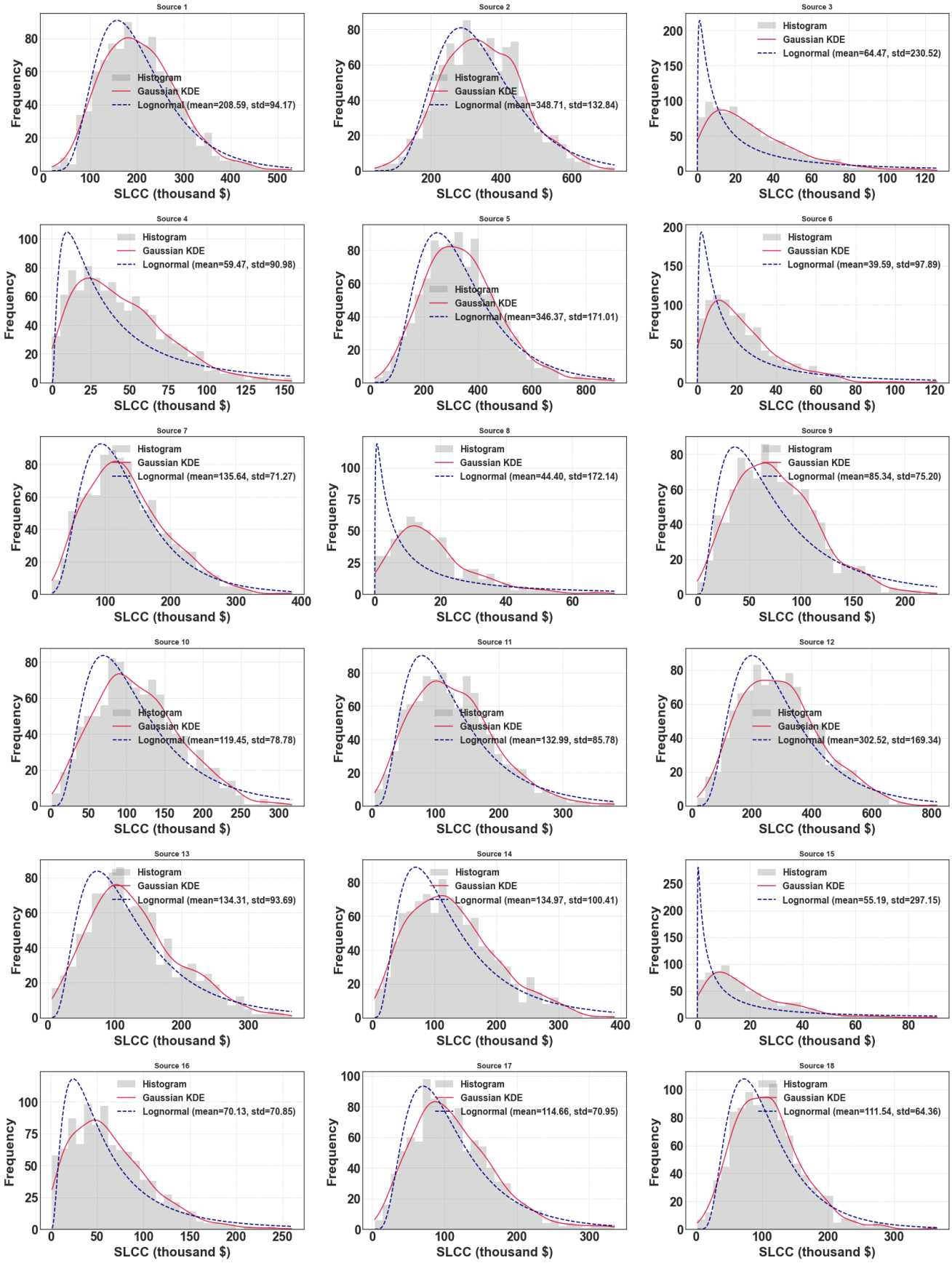


Fig. 8: Frequency distributions of the SLCC corresponding to the 18 individual hazard sources.

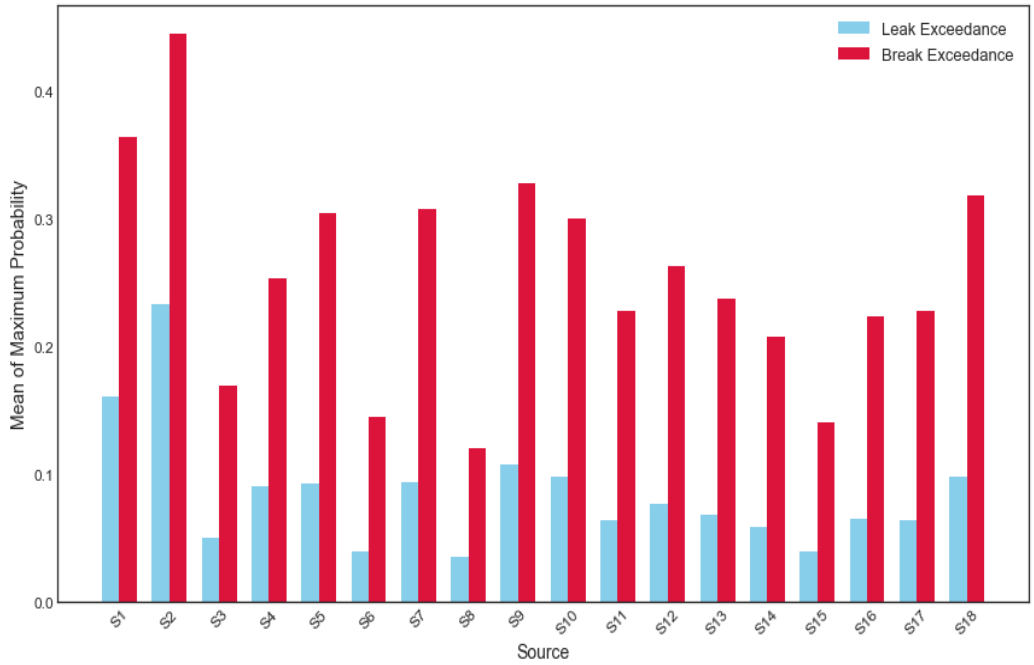


Fig. 9: Maximum leakage and breakage probability exceedance due to each seismic source

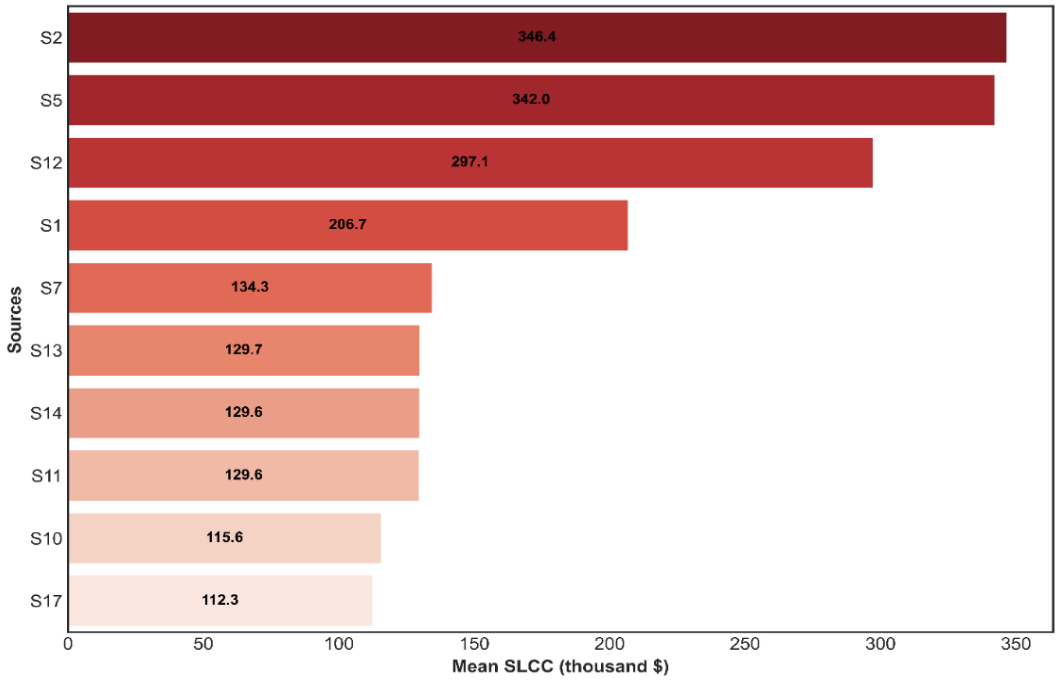


Fig. 10: Top 10 seismic sources ranked by mean SLCC

Figure 13a presents the exceedance probability for the pipeline considering the combined effects of all seismic sources, and Figure 13b shows the exceedance probabilities when the pipeline is affected individually by the 10 most influential seismic sources. Figure 13a indicates that the probability of exceeding SLCC above approximately $4 million is very low, while SLCC below $1 million occurs with relatively high probability. Comparing the two panels reveals that the combination of sources significantly increases the potential maximum SLCC. The combined scenario can result in SLCC exceeding $4.5 million, whereas no single source alone produces SLCC at this level.

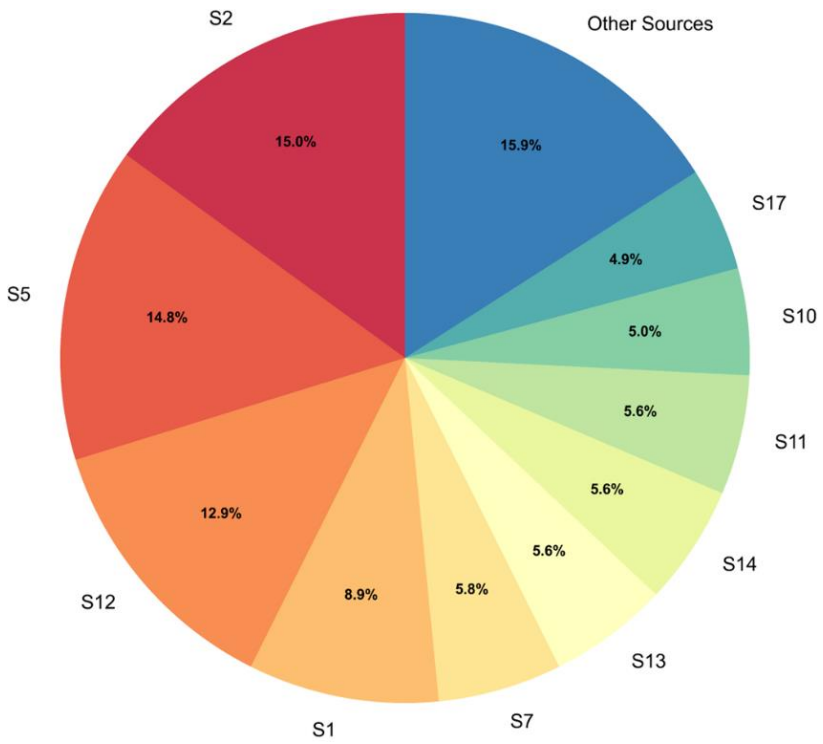


Fig. 11: Contribution of the top 10 seismic sources to the total SLCC

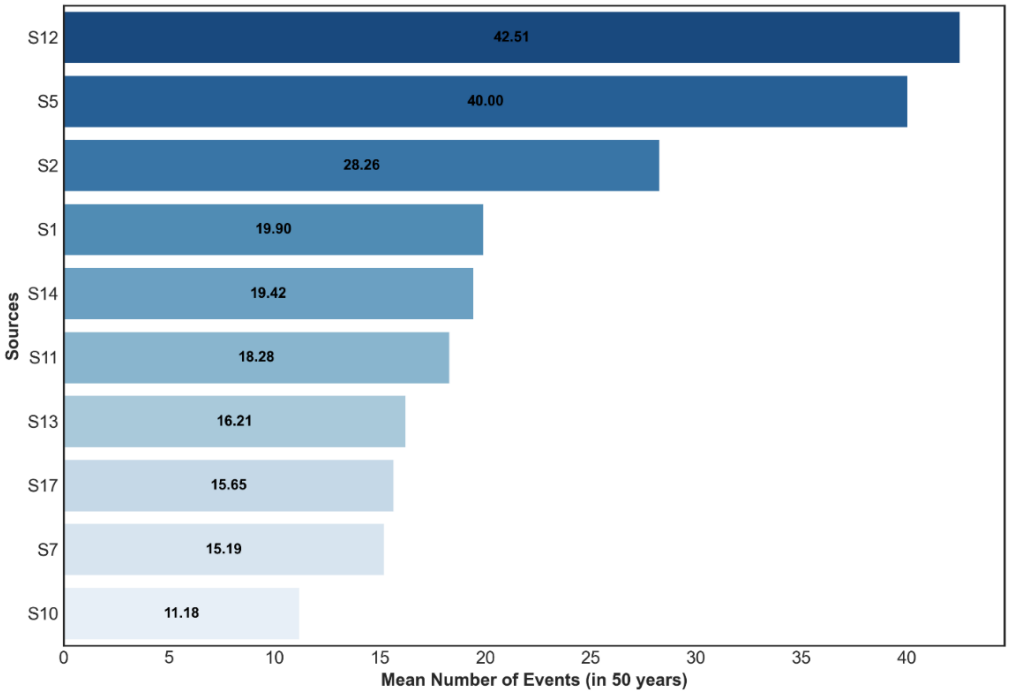


Fig. 12: Mean number of events for the top 10 seismic sources over the considered time period

In the final step, the SLCC distribution is examined with respect to the distance of seismic events from the pipeline alignment. The central section of the pipeline is adopted as a reference point to investigate how the SLCC varies along the pipeline. The resulting distance-dependent patterns are shown in Figure 14. As observed in the figure, costs increase over a certain distance range due to seismic conditions. For example, the average costs for distances less than 50 km are much lower than for distances up to 100 km.

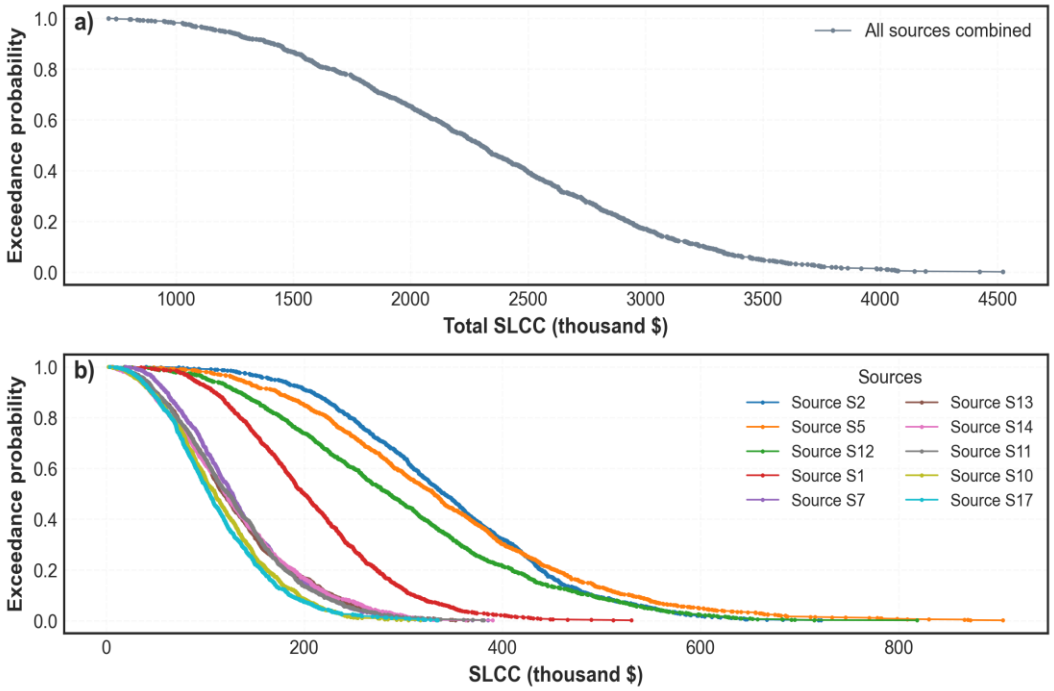


Fig. 13: Exceedance probability curve for buried pipeline SLCC: a) all sources combined, b) individual sources

Although the contribution of seismic sources and earthquakes at different distances helps to explain the main factors affecting the SLCC, a more detailed evaluation at the pipeline segment level is still required. This approach makes it possible to identify specific sections of the pipeline where higher SLCC values are more likely to occur. The results of segment-level evaluation are presented in Figure 15a.

Figure 15a presents the exceedance probability curves of the SLCC for all pipeline segments. The majority of segments (shown in gray) exhibit relatively low and tightly clustered cost ranges, with exceedance probabilities rapidly declining beyond approximately $25000 to $35000. In contrast, the highest-ranked segments show substantially higher and more widely distributed SLCC values. In particular, segments 106, 87, and 122 (Top 1–3) exhibit the highest potential costs and the longest right-skewed tails, suggesting a notable probability of costs exceeding approximately $60000 to $70000. The flatter slopes of these curves also indicate greater variability and uncertainty than the steeper curves observed for the other segments. Overall, Figure 15a highlights a clear separation between typical pipeline segments and a small number of high-impact segments that dominate the upper range of SLCC.

Figure 15b shows the spatial distribution of pipeline segments according to their mean SLCC. The top 10 highest-SLCC segments are not uniformly distributed along the pipeline but instead tend to cluster in certain areas, pointing to localized zones of greater seismic risk and damage potential. Although other segments may also warrant attention, this section focuses on these ten critical locations to help guide the prioritization of possible mitigation measures.

6. Discussion

The previous section presented a case study applying the proposed stochastic framework to estimate the SLCC of buried pipelines in a seismic region. The results show that the approach effectively captures SLCC under multiple hazards. This section interprets the results and discusses the advantages, limitations, and applicability of the method.

6.1 Results interpretation

To verify that the adopted number of Monte Carlo simulations provides statistically stable and reliable estimates of the SLCC metrics, a convergence analysis is conducted. To ensure statistical robustness of the Monte Carlo framework, the running mean and standard deviation of total SLCC are tracked as a function of simulation count (see Figure 16 for details). The results show that the mean total SLCC changes by only 0.34% between 700 and 1,000 simulations, while the standard deviation changes by just 0.03% over the final 300 simulations.

On the other hand, the quantile estimates stabilized after approximately 500 simulations, indicating convergence of the results. To further evaluate the stability of the upper tail, the second half of the simulations is resampled using a bootstrap procedure, and the coefficient of variation is computed for the 90%, 95%, 99%, and 99.5% quantiles. The

corresponding coefficient of variation values are 0.012, 0.021, 0.034, and 0.041. Since all values are below the 5% criterion, the tail of the SLCC distribution is considered adequately represented with 1,000 realizations. This confirms that 1,000 Monte Carlo simulations are sufficient for stable estimation of the primary SLCC metrics reported in this study.

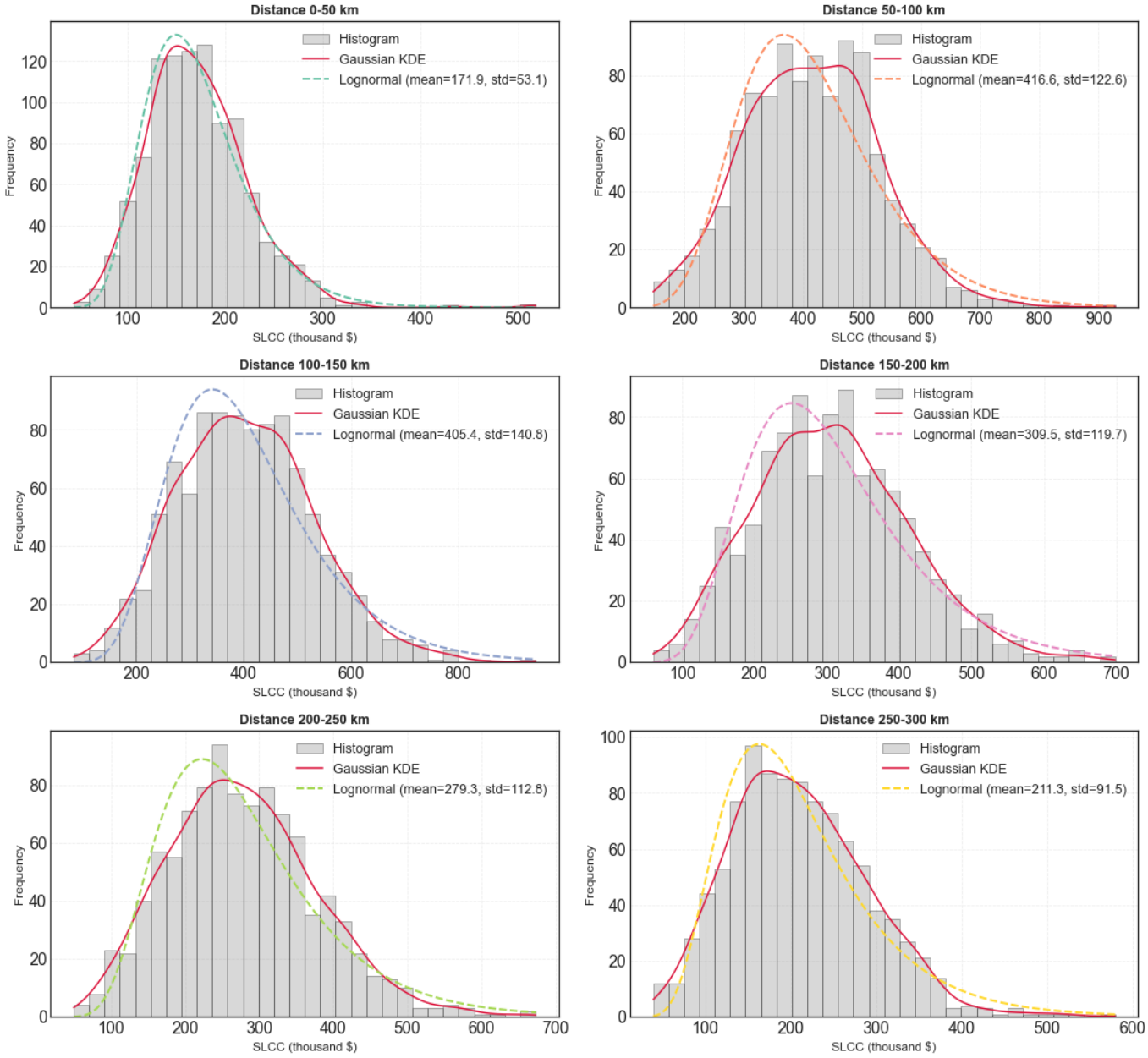


Fig. 14: Distance-dependent distribution of the SLCC along the buried pipeline

Based on the results shown in Figure 8, the SLCC values for all seismic sources exhibit a clear positive skew, with a long tail extending toward higher loss levels. This pattern reflects the inherent nature of earthquake-induced losses, where a small number of rare but severe events account for a substantial portion of the total damage. The fitted lognormal distribution closely reproduces both the central part of the distribution and its upper tail, supporting the suitability of the lognormal assumption for probabilistic SLCC modeling.

In addition, the sources display notable differences in both the mean and the spread of their SLCC distributions. Sources such as Source 1, Source 2, and Source 5 show higher mean SLCC and considerably wider variability, indicating greater uncertainty and a higher potential for extreme SLCC outcomes. In contrast, sources like Source 11 and Source 17 exhibit more concentrated and stable distributions, suggesting more predictable behavior. Together, these observations indicate that each seismic source differs not

only in its overall contribution to the total SLCC but also in the variability and reliability of the losses it generates. These differences suggest that seismic sources may contribute to the total SLCC either through frequent earthquake occurrences or through more serious damage per event. Clarifying this requires comparing each source's contribution to the total loss with its event frequency.

Figure 10 and Figure 12, respectively, illustrate the mean SLCC and the event frequency across the ten most influential seismic sources. However, considering these results separately does not clearly reveal whether the high total loss from a given source is mainly due to the large number of earthquakes it produces or to the particularly damaging nature of its individual events. To better link these results, an efficiency metric is introduced.

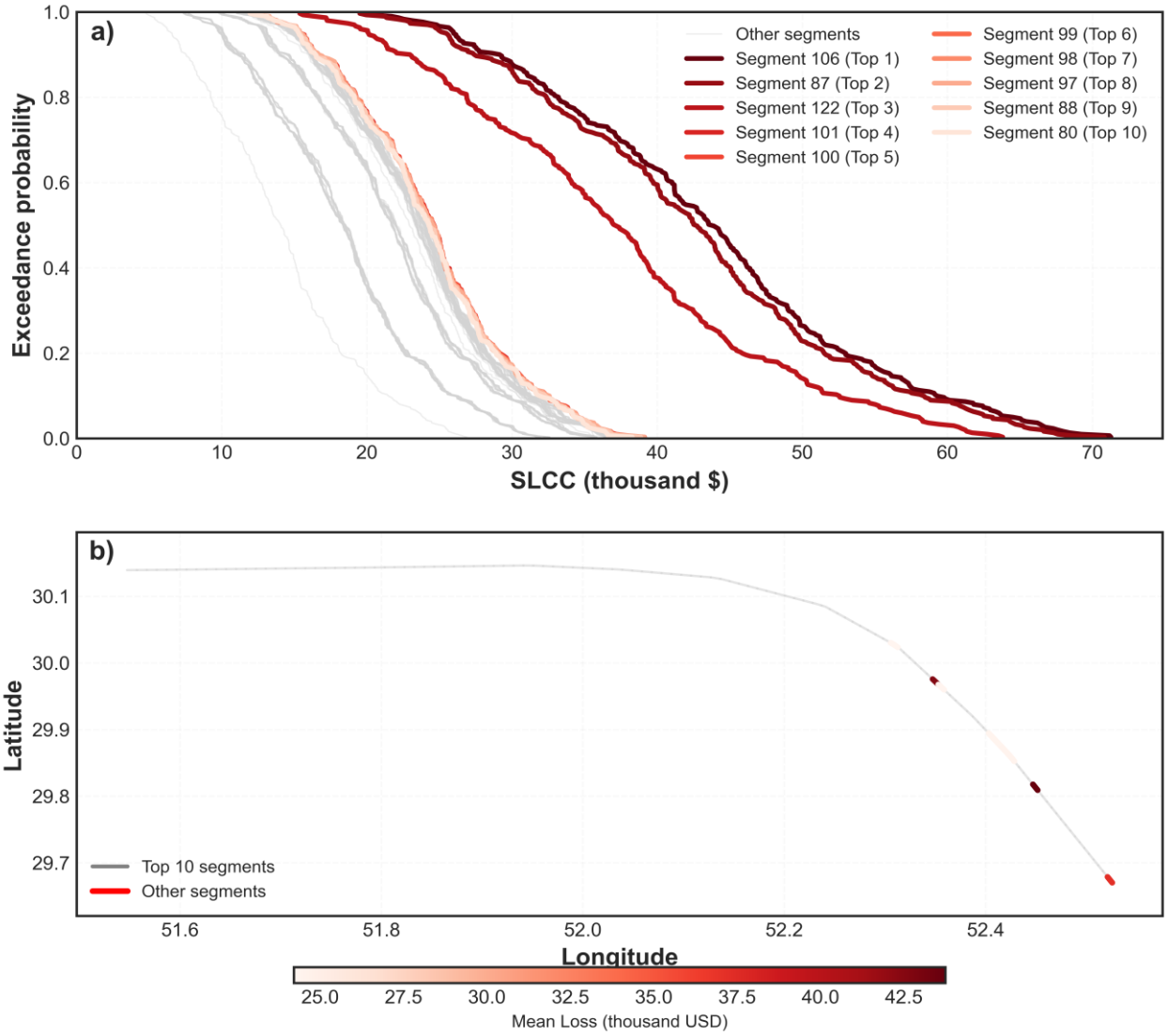


Fig. 15: SLCC of all segment pipeline: a) exceedance probability curves and b) identification of high SLCC locations

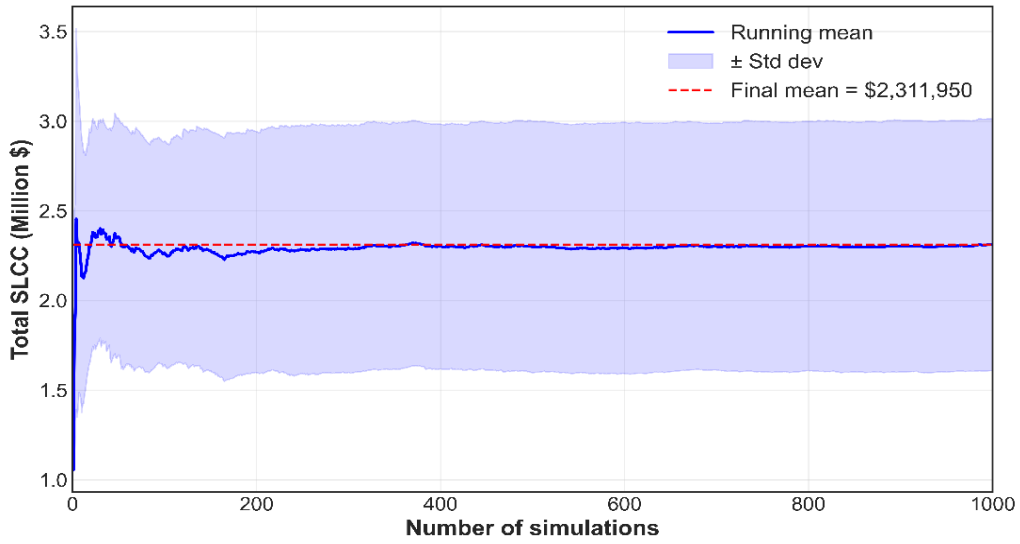


Fig. 16: Convergence analysis of Monte Carlo simulations for SLCC estimation

This metric represents the average damage produced by a typical earthquake from each source and reflects the relationship between the source's percentage contribution to the total SLCC and its event frequency, as shown in Figure 17. Among the ten sources, Source 2 shows the highest efficiency, indicating that earthquakes originating from this source tend to cause the largest average loss per event. In contrast, sources such as Source 12 and Source 5 occur more frequently but generally produce lower losses per event, suggesting that their overall contribution is mainly driven by recurrence rather than by the severity of individual events. On the other hand, seismic sources with similar efficiency values do not necessarily exhibit the same hazard characteristics. As shown in Figure 17, Sources 1 and 10 have nearly the same efficiency values, although their contributions to the SLCC differ noticeably. Source 10 accounts for about 5% of the total SLCC, whereas Source 1 contributes approximately 8.9%. This similarity in efficiency is mainly related to the difference in the mean occurrence rates of the two sources. As a result, despite their comparable efficiency values, the SLCC associated with Source 1 is nearly 44% greater than that of Source 10, as illustrated in Figure 11. This indicates that seismic sources with similar efficiency values may still correspond to notably different levels and characteristics of seismic hazard.

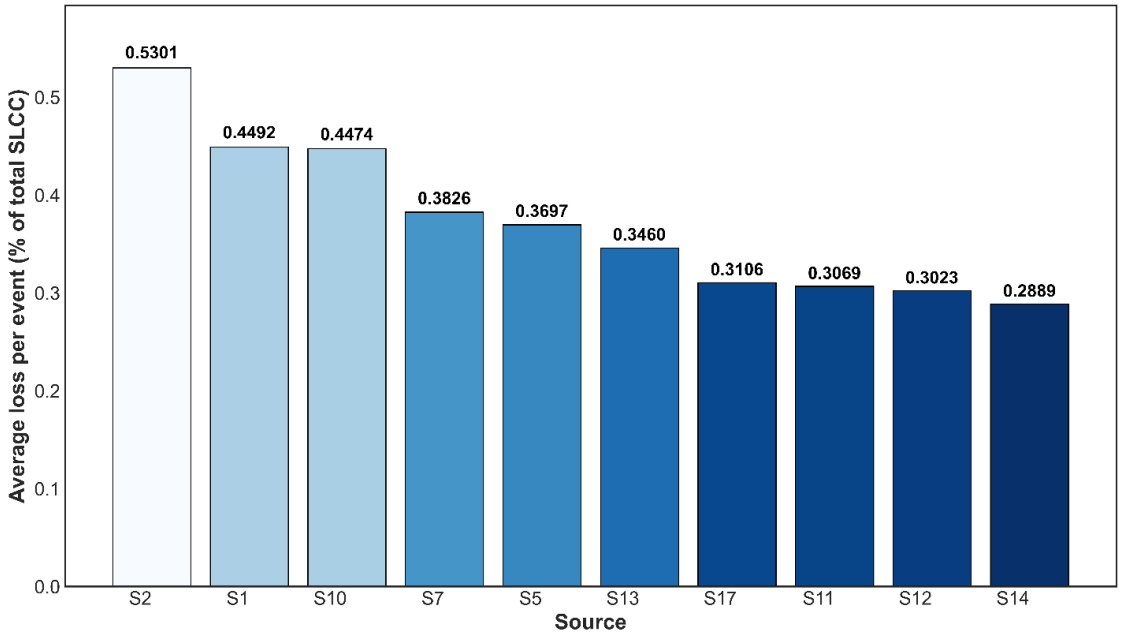


Fig. 17: Efficiency indicator for the most influential seismic sources

As shown in Figure 15b, the spatial distribution of mean SLCC along the pipeline highlights several segments with noticeably higher expected losses. This pattern reflects the non-uniform nature of seismic demand and structural vulnerability along the pipeline. Variations in ground conditions, proximity to active faults, site amplification effects, and local geometric or material changes can increase the damage potential in certain segments. Identifying these locations helps avoid overly generalized mitigation measures and allows strengthening, inspection, or replacement efforts to focus on the segments that contribute most to the total SLCC.

On the other hand, Monte Carlo simulations incorporate several sources of uncertainty to estimate the SLCC distribution. However, not all input parameters contribute equally to the variability of the total SLCC estimate. Identifying the most influential parameters is important for improving model reliability and guiding future data collection, especially when vulnerability and loss models are taken from external frameworks. In this study, R_R and damage ratios were adopted from HAZUS, which was originally developed using U.S. earthquake data. Although HAZUS is widely used for preliminary assessments, its direct application to Iranian gas pipelines may introduce bias due to differences in construction practices, soil conditions, repair costs, and post-earthquake recovery procedures. Because earthquake-induced pipeline damage data are very limited in the study region, and especially for the pipeline system considered here, direct validation of the model results is not possible. Therefore, sensitivity analysis is used as a practical approach to evaluate the robustness of the model and to identify the input parameters that most strongly influence the SLCC estimates.

In this study, a one-factor-at-a-time sensitivity analysis is conducted. Eight key parameters are examined by varying each one at three levels (low, baseline, and high) while keeping the others at their baseline values. The selected parameters and their ranges are taken directly from the computational framework and represent the main sources of epistemic uncertainty. Seismic hazard parameters are considered as multiplicative factors applied to the baseline values of each seismic source. In contrast, the seismic vulnerability parameters, specifically the coefficient (k) and exponent (Beta) in each vulnerability model, are varied independently. Damage ratio values for different damage states are also adjusted to reflect uncertainty in loss estimates. The variation ranges of all parameters are summarized in Table 4.

Table 4: Parameter ranges used in the one-factor-at-a-time sensitivity analysis

Parameter type	Parameter	Value	
		Minimum	Maximum
Seismic hazard	λ factor	0.75	1.25
	M_{max} factor	0.9	1.1
Seismic vulnerability	Beta-TGD	1.8	2.7
	Beta-PGD	0.2	0.5
	k-TGD	0.00005	0.001
	k-PGD	0.2	0.9
Seismic loss	Damage ratio 1	0.05	0.25
	Damage ratio 2	0.5	0.95

Figure 18 illustrates the sensitivity of total SLCC to variations in the main hazard, vulnerability, and loss parameters. Among all parameters, Damage ratio 2 shows the strongest influence, with SLCC changing from a substantial decrease (about −42%) to a moderate increase (+16%). This highlights the higher-damage-state ratio as a major source of uncertainty in total loss estimates. The λ factor, which scales seismic occurrence rates, also leads to notable changes in SLCC (−23% to +18%), underscoring the role of uncertainty in seismic activity rates. The M_{max} factor shows a moderate but noticeable effect, mainly lowering the loss estimates when its lower bound is applied. The vulnerability parameters Beta-PGD, Beta-TGD, and k-PGD have smaller and mostly negative effects. This indicates that although variations in R_R parameters affect the results, their influence is weaker than that of seismic hazard and damage ratio parameters. This negative trend is mainly related to the nonlinear behavior of R_R functions and the distribution of seismic hazard. Changes in these parameters tend to increase response dispersion and redistribute damage probabilities across intensity levels, rather than directly raising the mean damage. As a result, their effect on SLCC remains limited and may even slightly reduce the estimated mean value in some cases.

6.2 Strengths and practical implications of the proposed framework

The proposed framework improves SLCC assessment by using a stochastic, scenario-based representation of earthquake sequences. It links seismic hazard, damage, and cost within a unified probabilistic framework, translating multiple-source hazards into decision-relevant economic measures. This approach allows the assessment of both expected losses and the tail behavior of SLCC, which is important for capturing low-probability, high-consequence events. From an engineering decision-making perspective, the framework supports a shift toward performance-based and risk-informed design for buried pipelines. Rather than relying on conservative design scenarios alone, the probabilistic SLCC results allow engineers to balance safety, reliability, and cost over the pipeline's service life. This is especially useful for optimizing design parameters, material selection, and route planning in seismically active regions.

Economically, the framework supports a transition from deterministic cost estimation to risk-informed financial planning, where uncertainty is explicitly incorporated into investment and maintenance decisions. The probabilistic representation of SLCC allows stakeholders to evaluate trade-offs between upfront costs and long-term risk reduction, thereby enabling more efficient allocation of resources in large-scale infrastructure projects. In terms of broader applicability, the proposed methodology is not limited to gas pipelines but can be extended to other spatially distributed infrastructure systems exposed to natural hazards. Its structure is particularly well-suited for integration with geospatial analysis tools and optimization algorithms, making it a strong candidate for applications such as resilient infrastructure planning, network-level risk assessment, and hazard-informed routing of lifeline systems. Finally, the framework provides a foundation for future integration with more advanced components, such as indirect loss modeling, system-level interdependencies, and resilience-based performance metrics. This extensibility enhances its long-term relevance and positions it as a flexible platform for next-generation seismic risk assessment and infrastructure management.

6.3 Limitations and associated uncertainties

A key limitation of this study is the reliance on R_R and damage ratios from the HAZUS framework, which were originally developed for U.S. structural, geotechnical, and economic conditions. Although HAZUS is used primarily as a modeling tool here, all hazard inputs have been adjusted to reflect Iranian conditions, including probabilistic seismic hazard analysis with region-specific ground motion models and local susceptibility data for liquefaction and landslides. The R_R models, while not specifically calibrated for Iran, are chosen for their simplicity, broad acceptance, and consistency within probabilistic life cycle cost assessments. However, differences in local soil properties, construction techniques, pipeline installation, and regional cost factors may affect the accuracy of loss estimates. To address these uncertainties, a sensitivity analysis is performed by varying key parameters within realistic ranges, helping to assess the robustness of the framework despite limited local data. This approach allows for meaningful comparisons and improves confidence in the results despite inherent limitations.

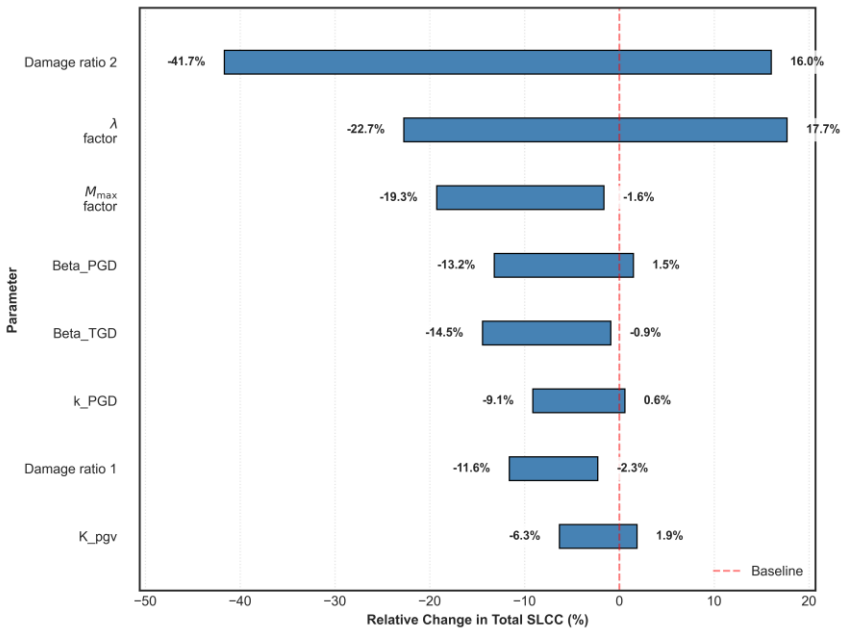


Fig. 18: Tornado plot of relative change in total SLCC for model input parameters

The modeling of different seismic sources, which is based on observations of actual events, introduces substantial uncertainty. Alternative modeling approaches could be considered to address this issue. In this study, the occurrence of TGD and PGD hazards is assumed to be independent; while this assumption simplifies the analysis and facilitates implementation, it also introduces additional uncertainty into the estimates. Although the framework partially captures this effect through the dependence of PGD probability on PGA within the PSHA, assuming independence between the hazards may still result in a slight underestimation of the overall seismic hazard [70]. Over time, phenomena such as corrosion can degrade the structural integrity of pipelines, potentially alter their seismic response, and influence the damage patterns. These factors warrant consideration in future research to improve the accuracy of seismic risk assessments.

Additionally, in the methodology, the loss of different scenarios is aggregated without considering the time of occurrence, which may affect their present value. Future studies could incorporate temporal discounting to reflect the time-dependent value of costs.

Another limitation of the present study is that the SLCC assessment focuses on direct repair costs associated with physical damage to the pipeline. Indirect consequences are not explicitly modeled. While these factors may contribute significantly to the total economic impact of major pipeline failures, their quantification requires detailed operational and socio-economic modeling. Future studies could integrate such factors within the proposed probabilistic framework to provide a more comprehensive estimation of SLCC. It should also be noted that operational and maintenance costs are not included in this study; accounting for these costs could further influence the results.

Overall, the proposed framework is flexible and can be extended to other infrastructure systems. Each step of the methodology can be adapted and refined to suit alternative modeling approaches or system types, offering a broad potential for future development.

7. Conclusion

This research presents a stochastic framework to evaluate the SLCC of buried pipelines, with particular emphasis on the simultaneous impact of TGD and PGD. By applying this methodology to a gas pipeline case study, the analysis captures the long-term economic consequences of various seismic scenarios while addressing the inherent uncertainties. The results demonstrate that total seismic losses do not stem from any single isolated factor. Instead, the final loss emerges from a complex interaction between the frequency of earthquake occurrence and the severity of the damage each event inflicts on the network. The following points detail the key conclusions of this study:

1. The results show that the probability of the SLCC exceeding $4 million is very small (below 5%), while losses under $1 million are highly likely (over 80%). These ranges give practical boundaries for financial planning. When all seismic sources are combined, the upper end of expected losses can rise above $4.5 million, higher than what any single source can produce alone.

2. The efficiency index reveals that Source 2 causes the largest damage per event despite its moderate occurrence rate. Although Source 12 occurs more frequently, its lower efficiency results in a substantially smaller contribution to the total losses. This indicates that source importance depends on both frequency and efficiency, rather than on either factor alone.

3. The distance analysis indicates that earthquakes occurring roughly 50–100 km from the pipeline generate higher losses than those at closer distances. This pattern reflects the combined effects of magnitude, site conditions, and near-field attenuation. It suggests that risk evaluation should identify a critical distance range rather than focusing only on the nearest sources.

4. The sensitivity analysis highlights the strong influence of the breakage damage ratio, where changes can shift the SLCC by about −42% to +16%. In comparison, the R_R parameters have much smaller effects and sometimes even reduce the estimated loss. This suggests that improving damage-ratio estimates is more important than fine-tuning R_R parameters.

Acknowledgments

The authors would like to express their heartfelt gratitude to their families for their unwavering support, patience, and encouragement throughout the course of this work.

Funding

The author(s) received no financial support for the research, authorship, and publication of this paper.

Declarations

The authors declare that they have no known competing financial interests or personal relationships that could have influenced the work reported in this paper.

Data availability

The data presented in this study are available on request from the corresponding author.

References

[1] Mirzaei H, Nasserasadi K. (2019) Fast seismic life cycle cost optimization of steel moment frames to improve seismic performance. KSCE Journal of Civil Engineering. 23(3): 1180-1189.

[2] Lee S H, An L-S, Kim H-K. (2025) Risk-based bridge life cycle cost and environmental impact assessment considering climate change effects. Scientific Reports. 15(1): 725.

[3] Omidian P, Khaji N. (2023) A total life-cycle cost–resilience optimization framework for infrastructures management using different retrofit strategies. Sustainable and Resilient Infrastructure. 8(6): 675-698.

[4] Iannacone L, Gardoni P. (2023) Physics-based repair rate curves for segmented pipelines subject to seismic excitations. Sustainable and Resilient Infrastructure. 8(1): 121-141.

[5] Alavi S H, Mashayekhi M, Zolfaghari M. (2024) Incorporating seismic risk assessment into the determination of the optimal route for gas pipelines. Sustainable and Resilient Infrastructure. 9(4): 328-348.

[6] Shojaeian A, Farahani S, Behnam B, Mashayekhi M R. (2021) Seismic Resilience Assessment of Tehran's Southern Water Transmission Pipeline Using GIS-based Analyses. Numerical Methods in Civil Engineering. 6(2): 93-106.

[7] Sarcheshmehpour M, Estekanchi H. Life cycle cost optimization of earthquake-resistant steel framed tube tall buildings. in Structures. 2021. Elsevier.

[8] Rao A, Dutta D, Kalita P, Ackerley N, Silva V, Raghunandan M, Ghosh J, Ghosh S, Brzev S, Dasgupta K. (2020) Probabilistic seismic risk assessment of India. Earthquake Spectra. 36(1_suppl): 345-371.

[9] Agbo S, Roy K, Adeeb S, Li Y. (2024) A systematic literature review on permanent ground deformation patterns imposed on buried steel pipelines. Journal of Pipeline Science and Engineering. 4(2): 100151.

[10] Pineda-Porras O, Najafi M. (2010) Seismic damage estimation for buried pipelines: Challenges after three decades of progress. Journal of Pipeline Systems Engineering and Practice. 1(1): 19-24.

[11] Adachi T, Ellingwood B R. (2009) Serviceability assessment of a municipal water system under spatially correlated seismic intensities. Computer-Aided Civil and Infrastructure Engineering. 24(4): 237-248.

[12] Bi K, Hao H, Li C, Li H. (2017) Stochastic seismic response analysis of buried onshore and offshore pipelines. Soil Dynamics and Earthquake Engineering. 94: 60-65.

[13] Duan L, Liao C, Jeng D, Chen L. (2017) 2D numerical study of wave and current-induced oscillatory non-cohesive soil liquefaction around a partially buried pipeline in a trench. Ocean Engineering. 135: 39-51.

[14] Liang J, Sun S. (2000) Site effects on seismic behavior of pipelines: a review. Journal of pressure vessel technology. 122(4): 469-475.

[15] Wang H, Bao R, Li J, Ren J, Yan W, Sun X, Song X, Zhu J, Chen Y, Yan Z. (2024) Failure analysis of buried pipelines under the action of oblique slip faults. Engineering Failure Analysis. 160: 108204.

[16] Xu R, Jiang R, Qu T-j. (2021) Review of dynamic response of buried pipelines. Journal of pipeline systems engineering and practice. 12(2): 03120003.

[17] Zahid U, Godio A, Mauro S. (2020) An analytical procedure for modelling pipeline-landslide interaction in gas pipelines. Journal of Natural Gas Science and Engineering. 81: 103474.

[18] Feng W, Huang R, Liu J, Xu X, Luo M. (2015) Large-scale field trial to explore landslide and pipeline interaction. Soils and Foundations. 55(6): 1466-1473.

[19] Castiglia M, Fierro T, Santucci de Magistris F. (2020) Pipeline Performances under Earthquake-Induced Soil Liquefaction: State of the Art on Real Observations, Model Tests, and Numerical Simulations. Shock and Vibration. 2020(1): 8874200.

[20] Toprak S, Nacaroglu E, van Ballegooy S, Koc A C, Jacka M, Manav Y, Torvelainen E, O'Rourke T D. (2019) Segmented pipeline damage predictions using liquefaction vulnerability parameters. Soil Dynamics and Earthquake Engineering. 125: 105758.

[21] Kongar I, Giovinazzi S, Rossetto T. (2017) Seismic performance of buried electrical cables: evidence-based repair rates and fragility functions. Bulletin of Earthquake Engineering. 15(7): 3151-3181.

[22] Jahangiri V, Shakib H. (2020) Reliability-based seismic evaluation of buried pipelines subjected to earthquake-induced transient ground motions. Bulletin of earthquake engineering. 18(8): 3603-3627.

[23] Toprak S, Taskin F. (2007) Estimation of earthquake damage to buried pipelines caused by ground shaking. Natural hazards. 40(1): 1-24.

[24] Choudhury D, Chaudhuri C H. (2023) A critical review on performance of buried pipeline subjected to pipe bursting and earthquake induced permanent ground deformation. Soil Dynamics and Earthquake Engineering. 173: 108152.

[25] Mousavi M, Hesari M, Azarbakht A. (2014) Seismic risk assessment of the 3rd Azerbaijan gas pipeline in Iran. Natural hazards. 74(3): 1327-1348.

[26] Alavi S H, Mashayekhi M, Zolfaghari M. (2025) Optimized seismic risk mitigation in pipeline routing using a metaheuristic GIS based approach. Scientific Reports. 15(1): 32916.

[27] Cheng X, Li Q, Hai R, Guo S, Xing X. (2024) Research progress and prospects of seismic performance on underground structure embedded in soft soil foundation. Scientific Reports. 14(1): 21883.

[28] Huang Y, Qin G, Yang M, Nogal M. (2025) Dynamic quantitative assessment of service resilience for long-distance energy pipelines under corrosion. Reliability Engineering & System Safety. 256: 110792.

[29] Alavi S H, Mashayekhi M. (2025) Development of a Seismic Life Cycle Cost Framework for Buried Pipelines. Reliability Engineering & System Safety: 111874.

[30] Kousar I, Alam M M. (2025) Review of wind and earthquake vibrations of skyscrapers: trend, cost, vibration, failure, maintenance, and vibration suppression techniques. Journal of Building Engineering: 114440.

[31] Shaw L, Orr N, Lawal H M, Briscoe S, Yan X, Coon J T, Melendez-Torres G, Martin-Pintado C, Garside R. (2025) Effectiveness of Interventions to Reduce Carbon-Emissions Within Secondary Healthcare: Systematic Review and Evidence and Gap Map. Campbell Systematic Reviews. 21(4): e70077.

[32] Adineh S, Behnam B, Tahershamsi A, Farahani S. (2025) Seismic Fragility in Life Cycle Cost Analysis for Gas Pipelines: Design and Cost Optimization Framework. Journal of Pipeline Science and Engineering: 100299.

[33] Baradaran Shoraka M, Yang T, Elwood K. (2013) Seismic loss estimation of non-ductile reinforced concrete buildings. Earthquake Engineering & Structural Dynamics. 42(2): 297-310.

[34] Dey S, Chakraborty S, Tesfamariam S. (2021) Multi-fidelity approach for uncertainty quantification of buried pipeline response undergoing fault rupture displacements in sand. Computers and Geotechnics. 136: 104197.

[35] Rayjada S P, Ghosh J, Raghunandan M. Seismic Life Cycle Cost Analysis of Indian RC Building Considering Hazard Uncertainty. in Symposium in Earthquake Engineering. 2022. Springer.

[36] Visini F, Carafa M M C, Valentini A, Di Naccio D, Kastelic V, Doglioni C. (2024) Scenario-based seismic hazard for horizontal and vertical ground motions in central Italy. Rendiconti Lincei. Scienze Fisiche e Naturali. 35(3): 563-582.

[37] Padgett J E, Dennemann K, Ghosh J. (2010) Risk-based seismic life-cycle cost–benefit (LCC-B) analysis for bridge retrofit assessment. Structural safety. 32(3): 165-173.

[38] Oleng M, Ozdemir Z, Pilakoutas K. (2025) Stochastic event-based probabilistic earthquake risk assessment framework for Uganda: towards informing the National Policy for Disaster preparedness and management. Bulletin of Earthquake Engineering. 23(4): 1371-1406.

[39] Karimzadeh S, Funari M F, Szabó S, Hussaini S S, Rezaeian S, Lourenço P B. (2024) Stochastic simulation of earthquake ground motions for the seismic assessment of monumental masonry structures: Source-based vs site-based approaches. Earthquake Engineering & Structural Dynamics. 53(1): 303-330.

[40] FEMA, Hazus Earthquake Model Technical Manual (Hazus 6.1). 2024, Federal Emergency Management Agency: Washington, DC.

[41] Baker J, Bradley B, Stafford P, Seismic hazard and risk analysis. 2021: Cambridge University Press.

[42] Bakhshi H, Alavi S M, Rezaie Z, Hassani M. (2022) Deterministic and Probabilistic Seismic Hazard Analysis of Petroleum Storage of Sabzevar. Journal of Rehabilitation in Civil Engineering. 10(2): 17-34.

[43] Farahani S, Behnam B, Tahershamsi A. (2020) Macrozonation of seismic transient and permanent ground deformation of Iran. Natural Hazards and Earth System Sciences. 20(11): 2889-2903.

[44] Nair G S, Dash S R, Mondal G. (2018) Review of pipeline performance during earthquakes since 1906. Journal of Performance of Constructed Facilities. 32(6): 04018083.

[45] Bommer J J, Alarcon J E. (2006) The prediction and use of peak ground velocity. Journal of Earthquake Engineering. 10(01): 1-31.

[46] Panah A, Farajzadeh M. Liquefaction susceptibility and opportunity macrozonation of Iran. in Proceedings of the fifth international conference on seismic zonation (Nice, October 17-19, 1995). 1996.

[47] Liao S S, Veneziano D, Whitman R V. (1988) Regression models for evaluating liquefaction probability. Journal of Geotechnical Engineering. 114(4): 389-411.

[48] ALA, Seismic fragility formulations for water systems part 1 guideline. 2001, ALA Washington, DC.

[49] O'Rourke M, Ayala G. (1993) Pipeline damage due to wave propagation. Journal of geotechnical engineering. 119(9): 1490-1498.

[50] Farahani S, Tahershamsi A, Behnam B. (2020) Earthquake and post-earthquake vulnerability assessment of urban gas pipelines network. Natural Hazards. 101(2): 327-347.

[51] Farahani S, Behnam B, Tahershamsi A. (2020) Probabilistic seismic multi-hazard loss estimation of Iran gas trunklines. Journal of Loss Prevention in the Process Industries. 66: 104176.

[52] Alavi S H, Bahrami A, Mashayekhi M, Zolfaghari M. (2024) Optimizing interpolation methods and point distances for accurate earthquake hazard mapping. Buildings. 14(6): 1823.

[53] FEMA, Hazus Inventory Technical Manual (Hazus 6.0). 2022, Federal Emergency Management Agency: Washington, DC.

[54] Lu K, Deng X, Jiang X, Cheng B, Tam V W. (2023) A review on life cycle cost analysis of buildings based on building information modeling. Journal of Civil Engineering and Management. 29(3): 268–288-268–288.

[55] Cardoni A, Elahi A R, Cimellaro G P. (2025) Seismic risk assessment of natural gas networks at the urban scale. International Journal of Disaster Risk Reduction: 105606.

[56] Rahimi H, Mahsuli M. (2019) Structural reliability approach to analysis of probabilistic seismic hazard and its sensitivities. Bulletin of Earthquake Engineering. 17(3): 1331-1359.

[57] Hosseini Y, Karami Mohammadi R. (2025) Seismic resilience optimization of urban transportation network during emergency medical response: A case study in Tehran metropolis. Numerical Methods in Civil Engineering. 9(3): 47-62.

[58] Tabandeh A, Sharma N, Gardoni P. (2022) Uncertainty propagation in risk and resilience analysis of hierarchical systems. Reliability Engineering & System Safety. 219: 108208.

[59] Assessment E S P. (2005) Pacific Earthquake Engineering Research Center. University of California, Berkeley.

[60] Gutenberg B, Richter C F. (1944) Frequency of earthquakes in California. Bulletin of the Seismological society of America. 34(4): 185-188.

[61] Pagani M, Monelli D, Weatherill G, Garcia J. (2014) Testing procedures adopted in the development of the hazard component of the OpenQuake engine. Global Earthquake Model (GEM) Technical Report. 9.

[62] Atkinson G M, Boore D M. (2006) Earthquake ground-motion prediction equations for eastern North America. Bulletin of the seismological society of America. 96(6): 2181-2205.

[63] Ghodrati Amiri G, Razeghi H, Razavian Amrei S, Aalaee H, Rasouli S. (2008) Seismic hazard assessment of Shiraz, Iran. Journal of Applied Sciences. 8(1): 38-48.

[64] Seismology I I o E E a, earthquake event record. 2022: Tehran, Iran.

[65] Mahsuli M, Rahimi H, Bakhshi A. (2019) Probabilistic seismic hazard analysis of Iran using reliability methods. Bulletin of Earthquake Engineering. 17(3): 1117-1143.

[66] Akkar S, Bommer J J. (2010) Empirical equations for the prediction of PGA, PGV, and spectral accelerations in Europe, the Mediterranean region, and the Middle East. Seismological Research Letters. 81(2): 195-206.

[67] Akkar S, Sandıkkaya M A, Bommer J J. (2014) Empirical ground-motion models for point-and extended-source crustal earthquake scenarios in Europe and the Middle East. Bulletin of earthquake engineering. 12(1): 359-387.

[68] Cornell C A, Banon H, Shakal A F. (1979) Seismic motion and response prediction alternatives. Earthquake Engineering & Structural Dynamics. 7(4): 295-315.

[69] Erdik M, Sesetyan K, Demircioglu M, Tuzun C, Giardini D, Gulen L, Akkar S, Zare M. Assessment of seismic hazard in the Middle East and Caucasus: EMME (Earthquake Model of Middle East) project. in Proc. of 15th World Conference on Earthquake Engineering. 2012.

[70] Psyrras N, Sextos A, Crewe A, Dietz M, Mylonakis G. (2020) Physical modeling of the seismic response of gas pipelines in laterally inhomogeneous soil. Journal of Geotechnical and Geoenvironmental Engineering. 146(5): 04020031.

This article is an open-access article distributed under the terms and conditions of the Creative Commons Attribution (CC-BY) license.